Computers and Chemical Engineering 174 (2023) 108229

Contents lists available at ScienceDirect

Computers and Chemical Engineering

journal homepage: www.elsevier.com/locate/compchemeng

Assessment of Lagrangean decomposition for short-term planning of integrated refinery-petrochemical operations

Ariel Uribe-Rodríguez [a,b], Pedro M. Castro [c,d], Gonzalo Guillén-Gosálbez [e], Benoît Chachuat [b,*]

[a] Colombian Petroleum Institute, ECOPETROL, Piedecuesta 681011, Colombia
[b] The Sargent Centre for Process Systems Engineering, Department of Chemical Engineering, Imperial College London, South Kensington Campus, London SW7 2AZ, United Kingdom
[c] Centro de Matemática Aplicações Fundamentais e Investigação Operacional, Faculdade de Ciências, Universidade de Lisboa, Lisboa 1749-016, Portugal
[d] Departamento de Engenharia Química, Instituto Superior Técnico, Universidade de Lisboa, Lisboa 1049-001, Portugal
[e] Department of Chemistry and Applied Biosciences, ETH Zürich, Institute for Chemical and Bioengineering, Vladimir-Prelog-Weg 1, Zürich 8093, Switzerland

ARTICLE INFO

Keywords:
Spatial Lagrangean decomposition
Large-scale nonconvex optimization
Integrated refinery-petrochemical complex
Short-term planning

ABSTRACT

We present an integrated methodology for optimal short-term planning of integrated refinery-petrochemical complexes (IRPCs) and demonstrate it on a full-scale industrial case study under four realistic planning scenarios. The large-scale mixed-integer quadratically constrained optimization models are amenable to a spatial Lagrangean decomposition through dividing the IRPC into multiple subsections, which comprise crude management, refinery, fuel blending, and petrochemical production. The decomposition algorithm creates virtual markets for trading crude blends and intermediate petrochemical streams within the IRPC and seeks an optimal tradeoff in such markets, with the Lagrange multipliers acting as transfer prices. The best results are obtained for decompositions with two or three subsections, achieving optimality gaps below 4% in all four planning scenarios. The Lagrangean decomposition provides tighter primal and dual bounds than the global solvers BARON and ANTIGONE, and it also improves the dual bounds computed using piecewise linear relaxation strategies.

1. Introduction

Integrated operations of petrochemical plants and crude oil refineries are more resilient to fluctuations in the hydrocarbons market compared to independent businesses for petrochemical commodities and fuels production. By-products or intermediate streams from the refinery can be transformed into added-value products at the petrochemical plant, while by-products from the petrochemical processes can improve fuel quality at the refinery side in return. The refinery can furthermore provide some of the natural gas required by steam crackers, while the petrochemical side can supply some of the hydrogen required by hydrotreatment units (Al-Qahtani and Elkamel, 2010, 2009, 2008; Ketabchi et al., 2019; Leiras et al., 2010). However, the planning of such integrated refinery-petrochemical complexes (IRPC) is challenging due to conflicting production targets for the various fuels and petrochemicals. Consequently, crude unloading and blending, crude separation trains and conversion processes, fuel blending, and petrochemical production need to be coordinated for maximizing the overall benefit of an IRPC instead of optimizing these operations separately (Jia and Ierapetritou, 2004; Méndez et al., 2006; Nasr et al., 2011).

The formulation of nonlinear models for parts of, or the whole, process network can enhance the prediction of yields and outlet stream properties from refining and petrochemical units. Pooling equations representing mixing operations with bilinear and trilinear terms as well as nonlinear blending rules to compute fuel specifications improve the predictive capability (Guerra et al., 2010). Models of crude distillation units (CDUs) also have a large impact on the predictive capability of the planning model, since CDUs provide all the intermediate streams for further processing in the downstream units and fuel blending. CDUs may be modeled by swing-cuts and micro-cuts, based on the true boiling point distribution (Kelly et al., 2014; Menezes et al., 2013; Wenkai et al., 2007; Zhang et al., 2001), surrogate models (López et al., 2013, 2012) and short-cut methods (Alattas et al., 2011).

Moro et al. (1998) formulated a nonlinear programming (NLP) model for a simplified refinery producing three grades of diesel. Nonlinearities in their model arose from modeling diesel hydrotreating, delay coking, fluid catalytic cracking (FCC), and diesel blending. Empirical correlations for the CDU and FCC were integrated into a small-scale refinery planning problem by Li et al. (2005). Later, Guerra

* Corresponding author.
E-mail address: b.chachuat@imperial.ac.uk (B. Chachuat).

https://doi.org/10.1016/j.compchemeng.2023.108229
Received 16 December 2022; Received in revised form 1 March 2023; Accepted 15 March 2023
Available online 21 March 2023
0098-1354/© 2023 The Author(s). Published by Elsevier Ltd. This is an open access article under the CC BY license (http://creativecommons.org/licenses/by/4.0/).

Nomenclature

Acronyms

BCS	base case scenario
CDU	atmospheric crude distillation unit
CL	clustering decomposition
CM	crude management
DRS	demand reduction scenario
FB	fuel blending
FCC	fluid catalytic cracking
HT	hydrotreating
HVGO	heavy vacuum gas oil
IRPC	integrated refinery-petrochemical complex
LB	lower bound on the optimal solution value
LD	Lagrangean decomposition
LCO	light cycle oil
LDS	logistic disruption scenario
LP	linear programming
MILP	mixed-integer linear programming
MINLP	mixed-integer nonlinear programming
MIQCQP	mixed-integer quadratically constrained quadratic program
MSS	multi-start strategy
NLP	nonlinear programming
S	total number of subproblems in each spatial Lagrangean decomposition scheme
OBBT	optimality-based bound tightening
PTQ	petrochemical
QCQP	quadratically constrained quadratic program
RB	refinery and fuel blending
REF	refinery
RPB	refinery petrochemical and fuel blending
SLP	successive linear programming
SQP	sequential quadratic programming
TAN	total acid number
UB	upper bound on the optimal solution value
WRPS	without integration refinery-petrochemical scenario

Sets

DC	domestic crude oils produced by different oil fields in Colombia
IC	imported crudes fed to the studied Colombian IRPC
E^{CB}	crude blends produced by crude management section
P^{CB}	crude blends volumetric composition or bulk properties (specific gravity, sulfur content, TAN)
E^{RP}	intermediate refined streams from REF to PTQ
P^{RP}	properties of the intermediate refined streams from REF to PTQ
E^{PR}	intermediate streams from PTQ to RB
P^{PR}	properties of the intermediate streams from PTQ to REF
E^{RB}	intermediate refined streams from REF to FB
P^{RB}	properties of the intermediate streams from REF to FB
E^{PB}	intermediate streams from PTQ to FB
P^{PB}	properties of the intermediate streams from PTQ to FB
X_{ij}	index of the complicating variables shared by subproblems i and $j > i$
V_i	complicating variables of subproblem i

Parameters

x^L, x^U	lower and upper bounds for variable x
α_v^{ij}	maximal step-size for linking variables v of the subproblems i and $j > i$
λ^L, λ^U	lower and upper bounds for Lagrange multiplier λ
Δ_v^{ij}	trust-region radius for linking variables v of the subproblems i and $j > i$

Binary variables

y	binary variable indicating the selection of operating conditions
y^i	binary variable belonging to subproblem i

Continuous variables

x	flowrates and stream properties
x^i	flowrates and streams properties belonging to subproblem i
v^i	relaxation of the bilinear terms
x_v^i	linking variables v of subproblem i (e.g. $QF_e^i, PF_{e,p}^i$)

Free variables

z^*	optimal solution value for monolithic problem P
z_λ^{LR}	optimal solution value for the Lagrangean relaxation LR_λ
$z_\lambda^{i,LD}$	optimal solution value for the subproblem i corresponding to LD_λ^i
$z^{DP,K}$	optimal solution value for the Lagrangean dual problem DP^K
λ_v^{ij}	Lagrange multiplier for linking variable v between subproblems i and j
η	auxiliary cost variable in Lagrangean dual problem DP^K

and Le Roux (2011a) optimized the same process network using surrogate models. Alhajri et al. (2008) addressed a more complex process topology, formulating polynomial surrogates for the catalytic reformer, FCC, hydrotreating and hydrocracking units. Although these modeling frameworks are able to represent complex process networks, their formulation leads to large-scale mixed-integer nonlinear programming (MINLP) models that are challenging to solve (Neiro and Pinto, 2004).

NLP models of industrial-sized refinery planning problems have been solved using local search methods such as successive linear programming (SLP) or successive quadratic programming (SQP) (ASPEN Technology Inc, 2010; Baker and Lasdon, 1985; Bonner and Moore, 1979; Haverly, 2015; Kutz et al., 2014), but even finding a feasible solution can prove challenging. A multi-start strategy (MSS) can sometimes overcome such feasibility and local optimality issues (Guerra et al., 2010; Guerra and Le Roux, 2011b), but it does not compute a dual bound, or offer mathematical guarantees of reaching a global optimum. Andrade et al. (2016) applied MSS to bilinear programming models and computed a dual bound by solving a linear programming (LP) relaxation based on the McCormick envelopes (McCormick, 1976), yet no procedure was implemented to refine this dual bound.

Siamizade (2019) formulated nonlinear process models with operating conditions such as reaction temperatures and severities as continuous decision variables based on commercial empirical correlations (Baird, 1987). The CDU was modeled with the Geddes fractionation-index method (Geddes, 1958; Gilbert et al., 1966), using binary variables to determine whether a component is in the stripping or rectifying section. The resulting MINLP model was solved by the state-of-the-art global optimizer BARON (Sahinidis, 2004), although the optimality gaps at termination were not reported. Li et al. (2016) presented a data-driven approach to optimize an IRPC using second-order polynomial correlations to predict yields and stream properties. The resulting mixed-integer quadratically constrained quadratic program (MIQCQP) was solved to global optimality using ANTIGONE (Misener and Floudas, 2014). A multiperiod extension to this problem was

recently addressed by Demirhan et al. (2020).

Castillo Castillo et al. (2017, 2018) also considered a MIQCQP formulation for refinery profit maximization and solved it to global optimality via a two-stage solution strategy that proved competitive with BARON and ANTIGONE. In the first stage, a mixed-integer linear programming (MILP) relaxation of the MIQCQP model was derived from piecewise McCormick envelopes (Castro, 2015; Castro et al., 2021; Gounaris et al., 2009; Karuppiah and Grossmann, 2006; Misener et al., 2011; Wicaksono and Karimi, 2008) or from the multiparametric disaggregation technique (Andrade et al., 2018; Castro, 2016; Castro and Grossmann, 2014; Kolodziej et al., 2013; Teles et al., 2013). A QCQP model obtained by fixing the binary variables of the MIQCQP model to the values from the solution of the MILP relaxation, was then solved to local optimality in the second stage. In cases where fixing the binaries did not compromise feasibility, this decomposition procedure could find solutions close to the global optimum. The iterative procedure for reducing the optimality gap worked by increasing the number of intervals in the partition for one of the variables in every bilinear term. The algorithm also employed optimality-based bound tightening (OBBT) (Castro and Grossmann, 2014; Puranik and Sahinidis, 2017) for reducing the domain of nonlinearly appearing variables. A drawback with this approach was that the first-stage MILP relaxation could already be computationally demanding to solve with just a few intervals in the partition, leading to high optimality gaps and poor initial points for the second-stage QCQP model.

1.1. Lagrangean decomposition in refinery planning

Neiro and Pinto (2004) proposed a general framework for modeling petroleum supply chains, where process units, tanks and pipelines are linked through intermediate streams coming from mixers and splitters. This formulation exhibits a block structure, which is amenable to a decomposition technique such as Lagrangean decomposition (LD) (Guignard and Kim, 1987). LD replaces the solution of a large optimization model by a series of smaller subproblems and updates the Lagrange multipliers connecting theses subproblems iteratively. In multi-plant, multiperiod production planning problems, both spatial and temporal decompositions may be developed. The former entails dualizing the mass balances around plants and markets, while the latter dualizes the inventory equations that connect variables in consecutive time periods. Jackson and Grossmann (2003) showed that the choice of complicating constraints to dualize can have a significant impact on computational performance and observed that temporal LD tends to provide tighter bounds. Neiro and Pinto (2006) applied temporal LD to solve a multiperiod single-refinery MINLP planning problem under uncertainty. Each realization of the uncertainty was given by a set of discrete scenarios comprising the crude oil procurement costs, product selling prices and demands. Then, a series of subproblems representing the combination of each time period and uncertainty scenario were solved iteratively and the Lagrange multipliers were updated using a subgradient method (Fisher, 1981). Zhao et al. (2017) presented a LD approach to solve a multiperiod MINLP planning problem for a petroleum refinery coupled with an ethylene plant, where the refinery sends fuel gas, ethane, propylene, naphtha, atmospheric gas oil and heavy gas oil to the ethylene plant, which provides hydrogen, residual fuel oil, and pyrolysis gasoline to the refinery in return. The decomposition strategy consisted of duplicating the variables of the material streams connecting the refinery and ethylene plant and dualizing the constraints equating both sets of variables. This resulted in a MILP subproblem for the refinery and a MINLP subproblem for the ethylene plant, which although simpler than the original model, remained challenging to solve to global optimality. The Lagrange multipliers were updated following the hybrid approach proposed by Mouret et al. (2011), which combines subgradient (Fisher, 1981), cutting planes (Cheney and Goldstein, 1959; Kelley, 1960) and trust-region (Marsten et al., 1975) methods.

Lagrangean decomposition has also been applied to integrate crude oil scheduling operations and refinery planning. Mouret et al. (2011) selected the CDU feedstock as the linking variable between the scheduling operations (MINLP subproblem) and refinery planning (NLP subproblem). For a given crude oil price, each subproblem could be solved independently to global optimality, making the spatial Lagrangean decomposition computationally tractable. Recently, Yang et al. (2020) proposed a multi-scale approach for the integration of a continuous-time MINLP model for crude oil scheduling and a discrete-time NLP for refinery planning, again using the hybrid approaches of Mouret et al. (2011) and Oliveira et al. (2013) to solve the dual subproblems.

1.2. Research gap and contribution

This paper presents a spatial Lagrangean-decomposition algorithm for the short-term planning of an industrial-scale IRPC. This algorithm is benchmarked against other solution strategies on an industrial case study that is more challenging and realistic than previous studies for the following reasons:

- A large variety of crude oils are considered, characterized by different volumes, qualities, and costs. These crudes are transported by pipeline or river fleet, depending on their geographic location, and can be blended to meet CDUs volume and quality specifications.
- Demands are defined on a large variety of fuel and petrochemical products, including five different grades of gasoline.
- Process units can operate in exclusive or non-exclusive campaigns. Specifically, the FCC units are constrained to a single operating mode during the whole planning horizon (to be decided by the optimization), while the CDUs can alternate between the maximization of medium distillates, paraffins or lubes, which represent different campaigns.
- The process network presents a high connectivity between units and intermediate streams. For instance, virgin naphtha can either be routed to gasoline blending, be a petrochemical feedstock, or be sold as an intermediate refined product.

All these features lead to a large-scale MIQCQP model with many nonconvex terms. It was recently tackled with a deterministic global optimization algorithm based on clustering decomposition (CL) (Uribe-Rodriguez et al., 2020) for a better performance than global solvers BARON and ANTIGONE. Still, the optimality gaps for several scenarios were above 10%, motivating the implementation of a spatial Lagrangean decomposition algorithm. To the best of our knowledge, this paper is the first to apply spatial LD to such a large-scale model. The novelty lies in formulating the decompositions for an industrial IRPC so that the optimality gaps can be reduced further.

The rest of the paper is organized as follows. Section 2 gives a brief description of the industrial case study. Section 3 details the three decomposition strategies, which consider the four separate IRPC sections: crude management, refinery, petrochemical production, and fuel blending; or three or two larger sections resulting first from the aggregation of refinery and fuel blending, and then from merging petrochemical production. Section 4 describes the Lagrangean decomposition algorithm, and the coordination between the sections subproblems, which involves iterating over the multipliers to generate a solution to the original problem. Section 5 presents the computational results for the different scenarios and decomposition strategies. Finally, Section 6 concludes the paper and discusses next research steps.

2. Industrial case study

The integrated refinery-petrochemical complex (IRPC) under consideration corresponds to one of the main facilities operating in the Colombian refining industry. It is composed of 60 industrial plants, represented by 125 models, and a tank farm for crude mixing and fuel blending consisting of 30 additional units. The IRPC is divided into four

sections: crude management, refinery, petrochemical production, and fuel blending. A brief description of each section is provided below. Further details can be found in Uribe-Rodriguez et al. (2020).

2.1. Crude management

Crude management involves procurement, transportation and blending of crude oils to produce streams with suitable bulk properties for feeding into the CDUs, such as sulfur content, API gravity and total acid number (TAN) (Guyonnet et al., 2009; Oddsdottir et al., 2013; Zhang et al., 2012). Crude oil characterization provides insight into potential economic and operational benefits. The gravity and sulfur content determine the market price, as crudes with low gravity and high sulfur content are cheaper than their high-density and low-sulfur counterparts. Thus, the crude oil management problem involves a tradeoff between the cost and quality of the blends.

Accounting for transportation enables a more realistic crude management operation. The logistics involves delivering batches of crude oil by pipeline and multimodal transport from oil fields, transport stations, and import ports to the refineries. As seen in Fig. 1, supply is given by domestic production of 17 different types of crude oil ($DC = \{DC1, \ldots, DC17\}$) geographically distributed across 8 regions in the country ($R = \{R1, \ldots, R8\}$). Domestic crude production ranges between 10 and 100 kbbl/day, for a total national production of 297 kbbl/day. A total of 7 imported crudes ($IC = \{IC1, \ldots, IC7\}$), up to a maximum of 15 kbbl/day per crude, complete the market availability. Domestic and imported crudes are delivered in batches through pipelines ($PL = \{PL3, \ldots, PL8\}$). Then, at the refinery, the 24 qualities of crude are combined into 9 crude blends ($E^{CB} = \{CB1, \ldots, CB9\}$); see Table 1 for the specifics. For instance, CB7 is obtained from domestic crudes DC1, DC4, DC7 −DC9, DC12, DC16 −DC17 and imported crudes IC1 − IC7. Note that crude blend CB9 was excluded from Table 1, as it is produced from crude blends CB1 − CB7.

2.2. Refinery

The refinery has a total capacity of 248 kbbl/day, distributed over 6 crude distillation units ($RCDU = \{RCDU1, \ldots, RCDU6\}$) that can operate in different campaigns during the planning horizon. Each campaign is represented by a logical unit (CDU), leading to 13 such logical CDUs ($CDU = \{CDU1, \ldots, CDU13\}$), each described by a specific set of constraints. As an example, RCDU1 has a processing capacity of 38 kbbl/day and can operate in 4 campaigns ($CDU1, \ldots, CDU4$), see Table 2.

The CDUs produce intermediate streams such as light ends (C1– C3), light and heavy naphtha, jet fuel, light and heavy diesel, atmospheric gas oil and reduced crude, which are either processed by refining downstream units or routed to fuel blending. Commodities $IR = \{Alkylate, GasOil\}$ can be imported as feedstock to certain refining units. The refinery also produces natural gas, ethane, olefins, virgin naphtha, and precursor materials for petrochemical production.

2.3. Petrochemical production

The petrochemical plant transforms ethane, olefins, and virgin naphtha to obtain added-value products such as polyethylene, propylene, benzene, and toluene. Several intermediate streams can be sold to the refinery for improving gasoline quality and specialty solvents production or supplying hydrogen to hydrotreating units. Relevant properties for these streams include their specific gravity, sulfur content, octane, Reid vapor pressure, and aromatics content.

2.4. Fuel blending

To produce fuels with the required quality, blenders can buy intermediate process streams from refinery and petrochemical production, complemented with refined products from domestic and international markets. Overall, 88 refined streams produce up to 22 fuel grades, with different quality specifications for each grade. A total of 25 streams are blended into 6 grades of medium distillates, which must comply with quality constraints on specific gravity, sulfur content, and cetane number. Two grades of jet fuel and four grades of diesel are produced as illustrated in Fig. 2. Diesel components from the CDUs provide one grade of diesel (Diesel4), while jet fuel components provide two grades of jet

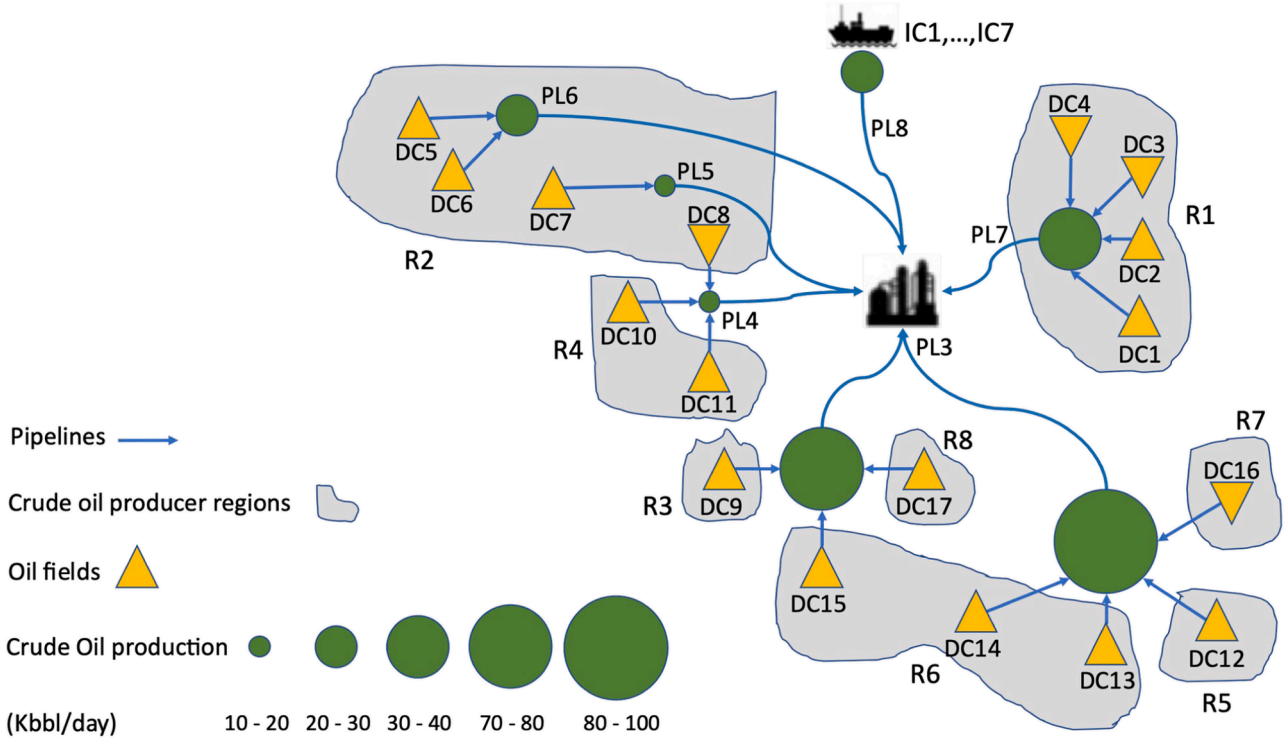

Fig. 1. Crude oil production and pipeline transportation network.

Table 1
Bulk properties and prices of domestic and imported crudes, and their incorporation into crude blends.

Crude Oil	Crude Blends								Bulk properties			Supply	
	CB1	CB2	CB3	CB4	CB5	CB6	CB7	CB8	API	Sulfur (%wt)	TAN (mg KOH/g crude)	Price*(USD/bbl)	Availability (kbbl/day)
DC1							x		24	1.218	1.135	39.50	2.1
DC2	x								29	0.515	0.097	49.70	31.1
DC3								x	32	0.812	0.168	49.68	3.4
DC4							x		20	1.934	0.528	35.43	2.2
DC5				x					28	0.642	1.494	45.27	5.6
DC6					x				23	0.929	2.139	41.26	24.2
DC7							x		22	1.008	2.300	40.28	12.6
DC8							x		19	0.957	3.126	38.50	5.8
DC9							x		20	1.129	3.341	34.57	71.7
DC10						x			26	1.223	1.680	42.49	3.3
DC11						x			23	1.239	2.642	40.13	3.7
DC12							x		19	1.848	0.122	40.86	32.0
DC13		x							44	0.306	0.093	52.00	24.1
DC14			x						45	0.048	0.070	52.11	26.7
DC15						x			24	0.984	0.468	42.78	13.5
DC16							x		18	1.140	0.137	30.77	16.5
DC17							x		20	1.139	2.381	35.08	18.9
IC1						x	x		39	0.156	0.629	52.23	15.0
IC2						x	x		39	0.921	0.060	52.30	15.0
IC3						x	x		29	0.246	0.590	49.28	15.0
IC4						x	x		29	0.690	1.266	49.17	15.0
IC5						x	x		29	0.605	0.470	49.15	15.0
IC6						x	x		40	0.482	0.043	52.37	15.0
IC7						x	x		34	0.158	0.605	50.64	15.0

* Pre-Covid-19 pandemic scenario with low crude oil prices.

Table 2
Set of logical units associated to each distillation column and corresponding processed crude blends.

	RCDU1				RCDU2	RCDU3	RCDU4	RCDU5			RCDU6		
Blend/CDU	1	2	3	4	5	6	7	8	9	10	11	12	13
CB1	x						x	x		x	x		x
CB2	x			x			x	x	x	x	x	x	x
CB3		x	x	x			x		x	x		x	x
CB4	x		x				x	x		x	x		
CB5	x		x				x	x					x
CB6	x						x	x			x		
CB7	x						x	x			x		
CB8	x		x				x	x		x	x		
CB9					x	x							
Capacity (kbbl/day)	38				52	27	39	55			37		

fuel (Jet1 & Jet2). Jet fuel components are also routed to the diesel pre-mix tank (Diesel pool). This tank also receives imported diesel, and other refinery streams such as hydrotreated diesel from the hydrotreating of heavy gas oil (HVGO HT), gas oil and heavy diesel pools. A second diesel grade with ultra-low sulfur (Diesel1) is obtained from hydrotreated diesel and diesel pre-mix blends. A fraction of the hydrotreated diesel is blended with heavy diesel from upstream refinery processes and light cycle oil (LCO) from FCC to produce two more diesel grades (Diesel2 & Diesel3).

3. IRPC decomposition

A monolithic model of the IRPC is too complex to be solved to global optimality using state-of-the-art solvers (Uribe-Rodriguez et al., 2020). Instead, the IRPC may be broken down into a number of sections in order to apply a Lagrangean decomposition approach. How to best decompose an IRPC is scenario-specific and remains an open question in general. Therefore, three different decompositions have been investigated in this work. Details about the mathematical formulations for each subproblem, information regarding availability, costs, and specifications for raw-materials and linking-streams, as well as the specifications and demands for the petrochemical and fuel products are provided in Sections 1–5 of the Electronic Supplementary Information.

3.1. Two sections: CM-RPB

The simplest decomposition entails a split between crude management (CM) on the one hand, and a merged section of refinery (REF), petrochemical (PTQ) and fuel blending (FB) on the other hand, denoted as RPB. Solving each of the two subproblems independently creates an imbalance between the flowrates, compositions and bulk properties of the crudes leaving the crude blend tanks and those reaching the CDU charge tanks (Fig. 3). In effect, the CM subproblem seeks to maximize profit by buying cheap crude oil from the market, minimizing the transportation cost to the refinery and selling crude blends at the highest price, regardless of the operational performance of the RPB section. Inversely, the RPB subproblem seeks to maximize profit by buying enough quantity of good-quality crude blends from CM at a cheap price, regardless of the costs incurred on the CM section by procuring and delivering the crudes.

Denoting by $e \in E^{\mathrm{CB}} := \{\mathrm{CB1}, \ldots, \mathrm{CB8}\}$ the process streams connecting CM to RPB, the linking variables consist of the flowrate QF_e^i and properties $PF_{e,p}^i$, with $i \in \{\mathrm{CM}, \mathrm{RPB}\}$ and index p representing either a bulk property (specific gravity, sulfur content, total acid number) or volumetric composition of the crude blend. The revenue of the CM section and cost of the RPB section associated to the linking streams can be computed as:

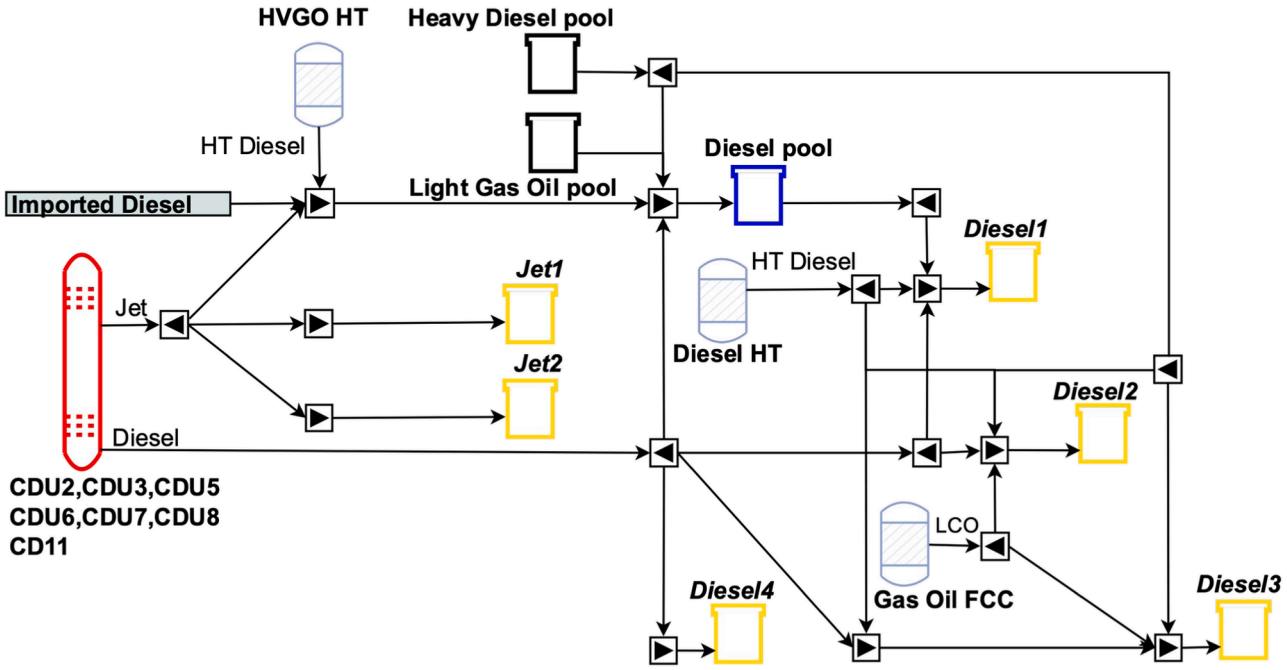

Fig. 2. Medium distillate blending.

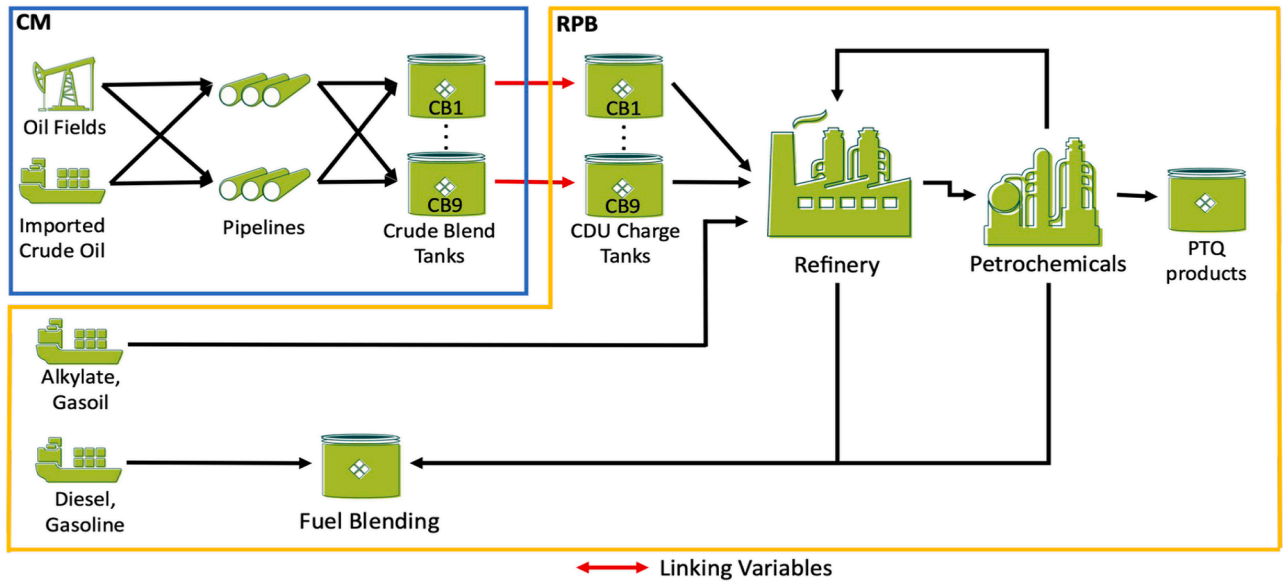

Fig. 3. Two-level decomposition between CM and RPB sections.

$$\text{revenue}^{\text{CM}} = \sum_{e\in E^{\text{CB}}} \lambda_e^{\text{CM,RPB}} \cdot QF_e^{\text{CM}} + \sum_{e\in E^{\text{CB}}} \sum_{p\in P^{\text{CB}}} \lambda_{e,p}^{\text{CM,RPB}} \cdot PF_{e,p}^{CM} \tag{1}$$

$$\text{cost}^{\text{RPB}} = \sum_{e\in E^{\text{CB}}} \lambda_e^{\text{CM,RPB}} \cdot QF_e^{\text{RPB}} + \sum_{e\in E^{\text{CB}}} \sum_{p\in P^{\text{CB}}} \lambda_{e,p}^{\text{CM,RPB}} \cdot PF_{e,p}^{\text{RPB}} \tag{2}$$

where the multipliers $\lambda_e^{\text{CM,RPB}}$ and $\lambda_{e,p}^{\text{CM,RPB}}$ act as the marginal prices for the availability and properties of a crude blend, respectively.

3.2. Three sections: CM-RB-PTQ

The next decomposition level entails three subproblems, crude management (CM), refinery (REF) merged with fuel blending (FB), denoted as RB, and petrochemicals (PTQ). The connecting streams between CM and RB are identical to those of the previous decomposition (Section 3.1 and Fig. 3). A second bidirectional market is created between RB, which sells materials for petrochemical production, and PTQ, which provides hydrogen to hydrotreating processes, raffinate for specialty solvent production, and components to improve gasoline quality (Fig. 4). The intermediate refined streams from RB to PTQ are $e \in E^{\text{RP}} := \{\text{CH}_4, \text{VirginNaphtha}, \text{Olefins}, \text{Ethylene}\}$ and from PTQ to RB are $e' \in E^{\text{PR}} := \{\text{H}_2, \text{GasolineComponents}, \text{Raffinate}\}$. Since, RB also buys crude blends from CM, the profit from RB is maximized when buying cheap precursor materials and selling their products at the highest possible price. In the same way, PTQ should buy natural gas, ethylene, olefins and virgin naphtha at the lowest possible cost, and it should sell hydrogen, raffinate and gasoline components at the highest possible price. The commodities QF_e^{RB} and QF_e^{PTQ} are traded at the price $\lambda_e^{\text{RB,PTQ}}$,

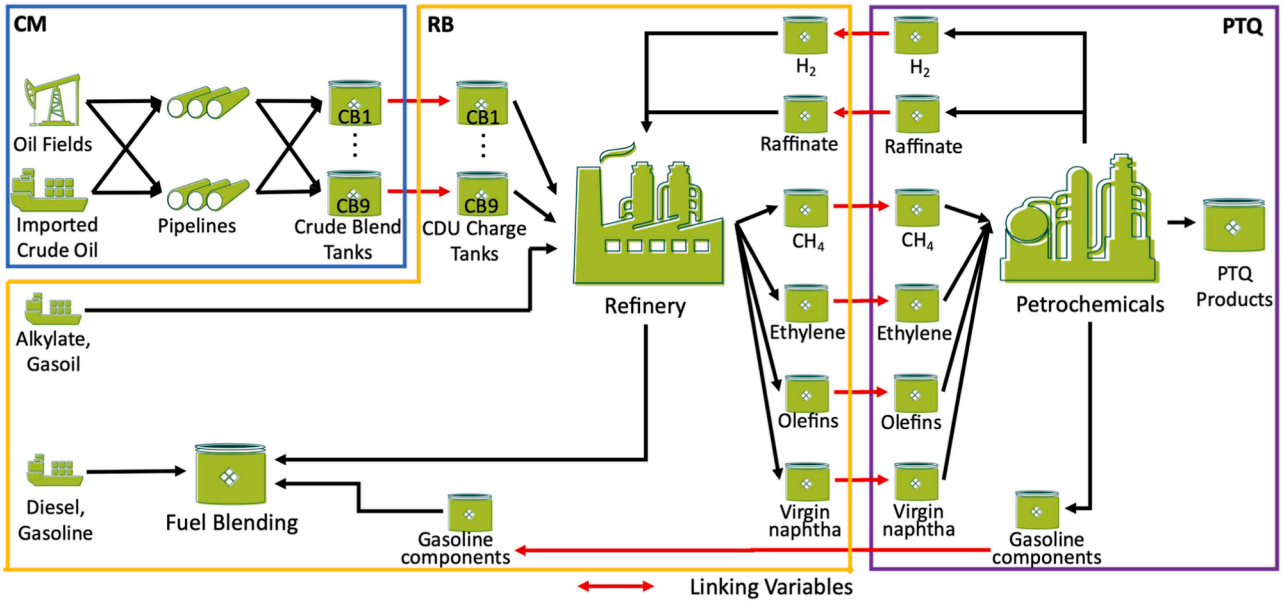

Fig. 4. Three-level decomposition between CM, RB and PTQ sections.

whereas $QF_{e'}^{\mathrm{RB}}$ and $QF_{e'}^{\mathrm{PTQ}}$ are negotiated at the price $\lambda_{e'}^{\mathrm{PTQ,RB}}$. There are also the penalty costs $\lambda_{e,p}^{\mathrm{RB,PTQ}}$ and $\lambda_{e',p'}^{\mathrm{PTQ,RB}}$ associated with the commodity qualities $PF_{e,p}^{\mathrm{RB}}$, $PF_{e,p}^{\mathrm{PTQ}}$, $PF_{e',p'}^{\mathrm{RB}}$ and $PF_{e',p'}^{\mathrm{PTQ}}$ for either the refinery properties $p \in P^{\mathrm{RP}}$ or the petrochemical properties $p' \in P^{\mathrm{PR}}$. Since the exchange between RB and PTQ is bidirectional, and recalling that RB also trades crude blends with CM, the revenues and costs can be computed as follows:

$$\mathrm{revenue}^{\mathrm{CM}} = \sum_{e\in E^{\mathrm{CB}}} \lambda_{e}^{\mathrm{CM,RB}} \cdot QF_{e}^{\mathrm{CM}} + \sum_{e\in E^{\mathrm{CB}}} \sum_{p\in P^{\mathrm{CB}}} \lambda_{e,p}^{\mathrm{CM,RB}} \cdot PF_{e,p}^{\mathrm{CM}} \tag{3}$$

$$\mathrm{revenue}^{\mathrm{RB}} = \sum_{e\in E^{\mathrm{RP}}} \lambda_{e}^{\mathrm{RB,PTQ}} \cdot QF_{e}^{\mathrm{RB}} + \sum_{e\in E^{\mathrm{RP}}} \sum_{p\in P^{\mathrm{RP}}} \lambda_{e,p}^{\mathrm{RB,PTQ}} \cdot PF_{e,p}^{\mathrm{RB}} \tag{4}$$

$$\mathrm{cost}^{\mathrm{PTQ}} = \sum_{e\in E^{\mathrm{RP}}} \lambda_{e}^{\mathrm{RB,PTQ}} \cdot QF_{e}^{\mathrm{PTQ}} + \sum_{e\in E^{\mathrm{RP}}} \sum_{p\in P^{RP}} \lambda_{e,p}^{\mathrm{RB,PTQ}} \cdot \mathrm{PF}_{e,p}^{\mathrm{PTQ}} \tag{5}$$

$$\mathrm{cost}^{\mathrm{RB}} = \mathrm{cost}^{\mathrm{CM,RB}} + \mathrm{cost}^{\mathrm{PTQ,RB}} \tag{6}$$

$$\mathrm{cost}^{\mathrm{CM,RB}} = \sum_{e\in E^{CB}} \lambda_{e}^{\mathrm{CM,RB}} \cdot QF_{e}^{\mathrm{RB}} + \sum_{e\in E^{CB}} \sum_{p\in P^{\mathrm{CB}}} \lambda_{e,p}^{\mathrm{CM,RB}} \cdot PF_{e,p}^{\mathrm{RB}} \tag{7}$$

$$\mathrm{cost}^{\mathrm{PTQ,RB}} = \sum_{e'\in E^{\mathrm{PR}}} \lambda_{e'}^{\mathrm{PTQ,RB}} \cdot QF_{e'}^{\mathrm{RB}} + \sum_{e'\in E^{\mathrm{PR}}} \sum_{p'\in E^{\mathrm{PR}}} \lambda_{e,p'}^{\mathrm{PTQ,RB}} \cdot PF_{e,p'}^{\mathrm{RB}} \tag{8}$$

$$\mathrm{revenue}^{\mathrm{PTQ}} = \sum_{e'\in E^{\mathrm{PR}}} \lambda_{e'}^{\mathrm{PTQ,RB}} \cdot QF_{e'}^{\mathrm{PTQ}} + \sum_{e'\in E^{\mathrm{PR}}} \sum_{p'\in E^{\mathrm{RP}}} \lambda_{e,p'}^{\mathrm{PTQ,RB}} \cdot PF_{e,p'}^{\mathrm{PTQ}} \tag{9}$$

3.3. Four sections: CM-REF-PTQ-FB

The final decomposition level additionally separates fuel blending (FB) from refining (REF), leading to four sections. REF can provide intermediate streams to FB, such as naphtha (inaphtha), jet (ijet), diesel (idiesel), and fuel (ifuel) generated from crude and vacuum distillation columns, catalytic processes such as hydrotreating and fluid catalytic cracking, thermal processes (e.g., visbreaking), and solvent extraction processes such as deasphalting, among others. The intermediate refined streams between REF and FB are $e \in E^{\mathrm{RB}} := \{\mathrm{inaphtha}, \mathrm{ijet}, \mathrm{idiesel}, \mathrm{ifuel}\}$ with properties $p \in P^{\mathrm{RB}} := \{\mathrm{SPG}, \mathrm{viscosity}, \mathrm{sulfur}, \mathrm{RON}, \mathrm{MON}, \mathrm{cetane}\}$. The commodities QF_{e}^{REF} and QF_{e}^{FB} are traded at the prices $\lambda_{e}^{\mathrm{REF,FB}}$, with penalty costs $\lambda_{e,p}^{\mathrm{REF,FB}}$ associated with the commodity qualities $PF_{e,p}^{\mathrm{REF}}$ and $PF_{e,p}^{\mathrm{FB}}$. In addition, FB receives gasoline components ($e' \in E^{\mathrm{PB}} := \{\mathrm{GasolineComponents}\}$, $p' \in P^{\mathrm{PB}} := \{\mathrm{SPG,sulfur,RON,MON}\}$) from PTQ (Fig. 5). The commodities $QF_{e'}^{\mathrm{PTQ}}$ and $QF_{e'}^{\mathrm{FB}}$ are traded at the prices $\lambda_{e'}^{\mathrm{PTQ,FB}}$, with penalty costs $\lambda_{e,p'}^{\mathrm{PTQ,FB}}$ associated with the commodity qualities $PF_{e,p'}^{\mathrm{PTQ}}$ and $PF_{e,p'}^{\mathrm{FB}}$.

The profit out of the PTQ section can be maximized by buying cheap natural gas, ethylene, olefins, and virgin naphtha from the refinery, while selling hydrogen, raffinate and gasoline components at a high price. The FB section receives gasoline components from PTQ and intermediate refined streams from REF. It can also operate as an import terminal, satisfying fuel demand regardless of REF and PTQ operations. Optimizing each section separately for given prices λ_{e}^{ij} of the traded commodities between sections $i,j \in \{\mathrm{CM,REF,PTQ,FB}\}$, with $i \neq j$, creates an imbalance between the flowrates QF_{e}^{i} and QF_{e}^{j} and the properties $PF_{e,p}^{i}$ and $PF_{e,p}^{j}$ as illustrated with the yellow circles in Fig. 6.

REF trades intermediate streams with CM, PTQ and FB, thereby making a profit by selling intermediate streams to PTQ ($\mathrm{revenue}^{\mathrm{REF,PTQ}}$) and FB ($\mathrm{revenue}^{\mathrm{REF,FB}}$). On the other hand, REF supports the costs of any crude blends traded with CM ($\mathrm{cost}^{\mathrm{CM,REF}}$) and of any intermediate streams received from PTQ ($\mathrm{cost}^{\mathrm{PTQ,REF}}$). The revenue for CM consists of the crude blends sold to REF.

$$\mathrm{revenue}^{\mathrm{REF}} = \mathrm{revenue}^{\mathrm{REF,PTQ}} + \mathrm{revenue}^{\mathrm{REF,FB}} \tag{10}$$

$$\mathrm{revenue}^{\mathrm{REF,PTQ}} = \sum_{e\in E^{\mathrm{RP}}} \lambda_{e}^{\mathrm{REF,PTQ}} \cdot QF_{e}^{\mathrm{REF}} + \sum_{e\in E^{\mathrm{RP}}} \sum_{p\in P^{\mathrm{RP}}} \lambda_{e,p}^{\mathrm{REF,PTQ}} \cdot PF_{e,p}^{\mathrm{REF}} \tag{11}$$

$$\mathrm{revenue}^{\mathrm{REF,FB}} = \sum_{e\in E^{\mathrm{RB}}} \lambda_{e}^{\mathrm{REF,FB}} \cdot QF_{e}^{\mathrm{REF}} + \sum_{e\in E^{\mathrm{RB}}} \sum_{p\in P^{\mathrm{RB}}} \lambda_{e,p}^{\mathrm{REF,FB}} \cdot PF_{e,p}^{\mathrm{RB}} \tag{12}$$

$$\mathrm{cost}^{\mathrm{REF}} = \mathrm{cost}^{\mathrm{CM,REF}} + \mathrm{cost}^{\mathrm{PTQ,REF}} \tag{13}$$

$$\mathrm{cost}^{\mathrm{CM,REF}} = \sum_{e\in E^{\mathrm{CB}}} \lambda_{e}^{\mathrm{CM,REF}} \cdot QF_{e}^{\mathrm{REF}} + \sum_{e\in E^{\mathrm{CB}}} \sum_{p\in P^{\mathrm{CB}}} \lambda_{e,p}^{\mathrm{CM,REF}} \cdot PF_{e,p}^{\mathrm{REF}} \tag{14}$$

$$\mathrm{cost}^{\mathrm{PTQ,REF}} = \sum_{e'\in E^{\mathrm{PR}}} \lambda_{e'}^{\mathrm{PTQ,REF}} \cdot QF_{e'}^{\mathrm{REF}} + \sum_{e'\in E^{\mathrm{PR}}} \sum_{p'\in P^{\mathrm{PR}}} \lambda_{e,p'}^{\mathrm{PTQ,REF}} \cdot PF_{e,p'}^{\mathrm{REF}} \tag{15}$$

$$\mathrm{revenue}^{\mathrm{CM}} = \sum_{e\in E^{\mathrm{CB}}} \lambda_{e}^{\mathrm{CM,REF}} \cdot QF_{e}^{\mathrm{REF}} + \sum_{e\in E^{\mathrm{CB}}} \sum_{p\in P^{\mathrm{CB}}} \lambda_{e,p}^{\mathrm{CM,REF}} \cdot PF_{e,p}^{\mathrm{REF}} \tag{16}$$

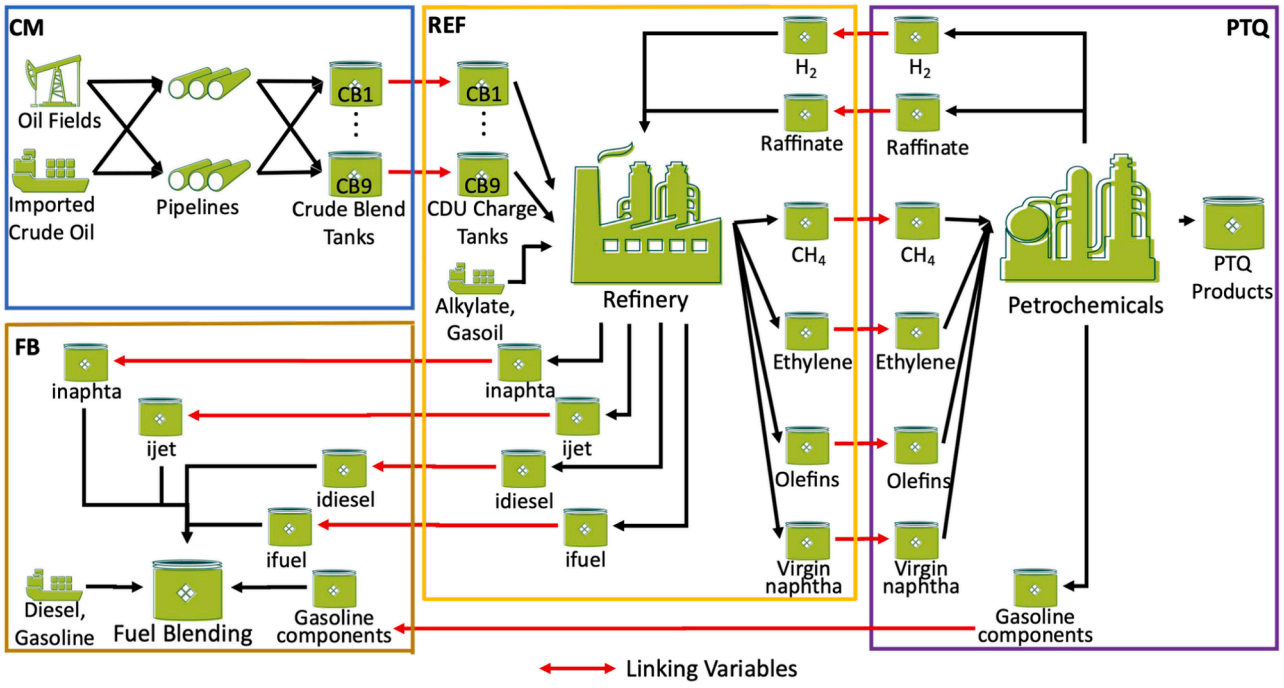

Fig. 5. Four-level decomposition between CM, REF, PTQ and FB sections.

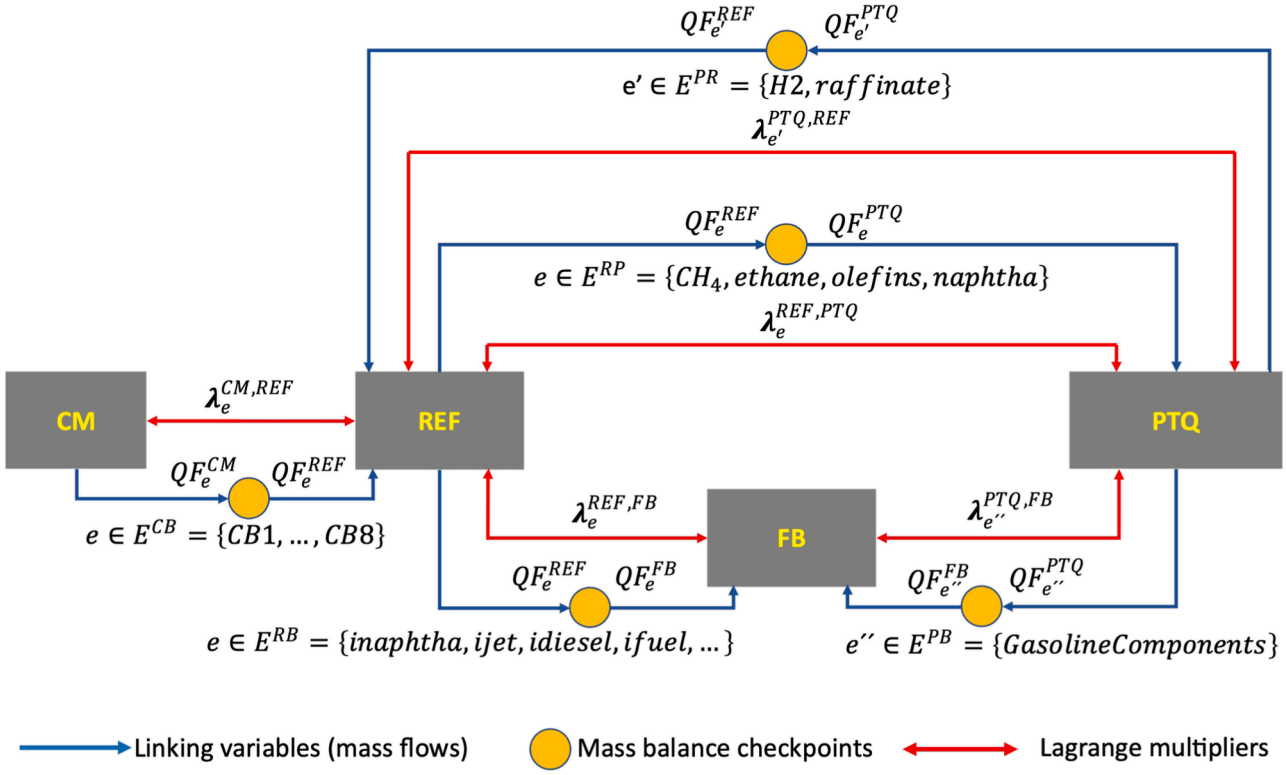

Fig. 6. Imbalances between the flows and properties from different sections in the four-level decomposition.

PTQ exchanges materials with REF and FB. The former entails a bidirectional trading between PTQ and REF, while PTQ sells components for the gasoline blending to FB in the latter. Thus, the revenue for PTQ results from trading gasoline components with FB ($\text{revenue}^{\text{PTQ,FB}}$) and from selling other streams to REF ($\text{revenue}^{\text{PTQ,REF}}$). On the other hand, the cost of PTQ (cost^{PTQ}) is incurred by the procurement of intermediate product streams from REF.

$$\text{revenue}^{\text{PTQ}} = \text{revenue}^{\text{PTQ,REF}} + \text{revenue}^{\text{PTQ,FB}} \tag{17}$$

$$\text{revenue}^{\text{PTQ,REF}} = \sum_{e' \in E^{\text{PR}}} \lambda_{e'}^{\text{PTQ,REF}} \cdot QF_{e'}^{\text{PTQ}} + \sum_{e' \in E^{\text{PR}}} \sum_{p' \in P^{\text{PR}}} \lambda_{e,p'}^{\text{PTQ,REF}} \cdot PF_{e,p'}^{\text{PTQ}} \tag{18}$$

$$\text{revenue}^{\text{PTQ,FB}} = \sum_{e' \in E^{\text{PB}}} \lambda_{e'}^{\text{PTQ,FB}} \cdot QF_{e'}^{\text{PTQ}} + \sum_{e' \in E^{\text{PB}}} \sum_{p' \in P^{\text{PB}}} \lambda_{e',p'}^{\text{PTQ,FB}} \cdot PF_{e',p'}^{\text{PTQ}} \tag{19}$$

$$\text{cost}^{\text{PTQ}} = \sum_{e \in E^{\text{RP}}} \lambda_{e}^{\text{REF,PTQ}} \cdot QF_{e}^{\text{PTQ}} + \sum_{e \in E^{\text{RP}}} \sum_{p \in P^{\text{RP}}} \lambda_{e,p}^{\text{REF,PTQ}} \cdot PF_{e,p}^{\text{PTQ}} \tag{20}$$

Finally, FB buys streams for fuel blending from both REF ($\text{cost}^{\text{REF,FB}}$) and PTQ ($\text{cost}^{\text{PTQ,FB}}$).

$$\text{cost}^{\text{FB}} = \text{cost}^{\text{REF,FB}} + \text{cost}^{\text{PTQ,FB}} \tag{21}$$

$$\text{cost}^{\text{REF,FB}} = \sum_{e \in E^{\text{RB}}} \lambda_{e}^{\text{REF,FB}} \cdot QF_{e}^{\text{FB}} + \sum_{e \in E^{\text{RB}}} \sum_{p \in P^{\text{RB}}} \lambda_{e,p}^{\text{REF,FB}} \cdot PF_{e,p}^{\text{FB}} \tag{22}$$

$$\text{cost}^{\text{PTQ,FB}} = \sum_{e' \in E^{\text{PB}}} \lambda_{e'}^{\text{PTQ,FB}} \cdot QF_{e'}^{\text{FB}} + \sum_{e' \in E^{\text{PB}}} \sum_{p' \in P^{\text{PB}}} \lambda_{e',p'}^{\text{PTQ,FB}} \cdot PF_{e',p'}^{\text{FB}}, \tag{23}$$

4. Mathematical framework

Short-term planning optimization of an IRPC can be cast as the following MIQCQP:

$$\begin{aligned} & z^* := \max f_0(x,y) \\ \text{s.t. } & f_m(x,y) \le 0 \ \forall m \in \{1,\cdots,M\} \\ & x \in [x^{\text{L}}, x^{\text{U}}] \subseteq \mathbb{R}^p_+, \ y \in \{0,1\}^q \end{aligned} \tag{P}$$

where z^* is the maximum profit, x is a p-dimensional vector of non-negative continuous variables (flows and properties of streams) constrained between lower x^{L} and upper x^{U} bounds, and y is a q-dimensional vector of binary variables used to select process operating conditions such as high, medium, and low severity in fluid catalytic process. The functions $f_m : \mathbb{R}^p \times \mathbb{R}^q \to \mathbb{R}$ in the objective function and constraints of P are quadratic in x and linear in y:

$$f_m(x,y) := \sum_{(r,s) \in \text{BL}_m} a_{rsm} x_r x_s + B_m x + C_m y + d_m \forall m \in \{0,\cdots,M\},$$

where BL_m is an index set of participating bilinear terms, a_{rsm} and d_m are scalars, and B_m and C_m are row vectors.

4.1. Lagrangean decomposition and relaxation

The reformulation P' of problem P for a set of $S > 1$ subproblems entails duplicating the continuous variables describing the connecting streams between sections and assigning them to different sets of constraints (Grossmann, 2021; Guignard and Kim, 1987). A few of these duplicated variables are displayed next to the mass balance checkpoints represented as yellow circles in Fig. 6 (e.g., the flowrates QF_e^{REF} and QF_e^{FB} of every stream e linking the refinery and fuel blending section). Formally, problem P' is made equivalent to P by adding the constraint $x_v^i = x_v^j \ \forall i,j > i, v \in X_{ij}$, where X_{ij} is the index set of the complicating variables (flowrates and properties) of all streams linking subproblems i and j.

$$\begin{aligned} & z^* := \max f_0(x,y) \\ \text{s.t. } & f_{m_i}^i(x^i,y^i) \le 0 \ \forall i \in \{1,\cdots,S\}, m_i \in \{1,\cdots,M\} \\ & x_v^i - x_v^j = 0 \quad \forall i,j \in \{1,\cdots,S\}, i<j, v \in X_{ij} \\ & x \in [x^{\text{L}}, x^{\text{U}}] \subseteq \mathbb{R}^p_+, y \in \{0,1\}^q \end{aligned} \tag{$P\prime$}$$

Each of the M constraints is allocated to a given subproblem, and the objective function is summing the objective terms of all the subproblems, with x^i and y^i denoting the vectors of continuous and binary variables that participate in subproblem i, respectively. The problem reformulation P' makes it possible to apply a solution strategy based on Lagrangean decomposition. In particular, a Lagrangean relaxation (Guignard, 2003; Guignard and Kim, 1987) LR_λ of problem P' can be obtained by transferring into the objective function the complicating constraints $x_v^i = x_v^j$ multiplied by their Lagrange multipliers λ_v^{ij}, which can either take positive or negative values:

$$\begin{aligned} & z_\lambda^{LR} := \max \sum_{i=1}^{s} f_0^i(x^i,y^i) + \sum_{i=1}^{S-1} \sum_{j=i+1}^{S-1} \sum_{v \in X_{ij}} \lambda_v^{ij}(x_v^i - x_v^j) \\ \text{s.t. } & f_{m_i}^i(x^i,y^i) \le 0 \ \forall i \in \{1,\cdots,S\}, m_i \in \{1,\cdots,M\} \\ & x \in [x^{\text{L}}, x^{\text{U}}] \subseteq \mathbb{R}^p_+, y \in \{0,1\}^q \end{aligned} \tag{LR_λ}$$

For fixed values of the multipliers λ_v^{ij}, problem LR_λ can be decomposed into S parametric optimization problems, which are solved independently from one another:

$$\begin{aligned} & z_\lambda^{i,\text{LD}} := \max f_0^i(x^i,y^i) + \sum_{j=i+1}^{S} \sum_{v \in X_{ij}} \lambda_v^{ij} x_v^i - \sum_{j=1}^{i-1} \sum_{v \in X_{ji}} \lambda_v^{ji} x_v^i \\ \text{s.t. } & f_{m_i}^i(x^i,y^i) \le 0 \ \forall m_i \in \{1,\cdots,M\} \\ & x^i \in [x^{\text{L}}, x^{\text{U}}] \subseteq \mathbb{R}^p_+, \ y \in \{0,1\}^q \end{aligned} \tag{LD_λ^i}$$

Therefore, $z_\lambda^{\text{LD}} := \sum_{i=1}^{S} z_\lambda^{i,\text{LD}}$ provides an upper bound on the optimal value z^* of problem P.

4.2. Dual problem

A standard practice is to solve a Lagrangean dual problem for determining values of the multipliers λ_v^{ij} that minimize the upper bound z_λ^{LD} from Lagrangean relaxation (Grossmann, 2021). Grossmann and co-workers (Mouret et al., 2011; Oliveira et al., 2013; Yang et al., 2020) developed a hybrid method for updating the Lagrange multipliers by combining a subgradient method (Held et al., 1974; Held and Karp, 1971) with a cutting plane approach (Cheney and Goldstein, 1959), trust-region method (Marsten et al., 1975) and volume algorithm (Barahona and Anbil, 2000). Specifically, at a given iteration $K > 0$ the following LP is solved to update the Lagrange multipliers $\lambda_v^{ij,K}$ that feed into subproblem LD_λ^i at the next iteration $(K+1)$:

$$\begin{aligned} & z_K^{DP} := \min \ \eta \\ \text{s.t. } & \eta \ge \bar{f}_k(\lambda_v^{ij,k}) \ \forall k \in \{1,\cdots,K\} \\ & \left|\lambda_v^{ij,K} - \lambda_v^{ij,K-1}\right| \le \Delta_v^{ij}, \lambda_v^{ij,K} \in [\lambda^{\text{L}}, \lambda^{\text{U}}] \forall i,j \in \{1,\cdots,S\}, \ i<j, \ v \in X_{ij} \end{aligned} \tag{DP^K}$$

where the main decision variables are the Lagrange multipliers $\lambda_v^{ij,K}$ within the range $[\lambda^{\text{L}}, \lambda^{\text{U}}]$, $\lambda_v^{ij,K-1}$ are the values of the Lagrangean multipliers computed at the previous iteration $K-1$, and the augmented objective function $\bar{f}_k$ is given by:

$$\bar{f}_k(\lambda_v^{ij,k}) := \sum_{i=1}^{S} \left[f_0^i(x^{i,k}, y^{i,k}) + \sum_{j=i+1}^{S} \sum_{v \in X_{ij}} \lambda_v^{ij,k} x_v^{i,k} - \sum_{j=1}^{i-1} \sum_{v \in X_{ji}} \lambda_v^{ji,k} x_v^{i,k} \right] \tag{24}$$

with $x^{i,k}$ and $y^{i,k}$ taking the optimal solution of subproblem LD_λ^i at iteration k.

In practice, the variability of z_λ^{LD} between iterations may be reduced by adjusting the trust-region radius Δ_v^{ij} of the Lagrange multipliers $\lambda_v^{ij,K}$ around $\lambda_v^{ij,K-1}$, before solving DP^K (Oliveira et al., 2013; Barahona and Anbil, 2000). The procedure used herein consists of determining an average deviation between the optimal values $x_v^{i,K}$ of the complicating variables in subproblem LD_λ^i at iteration K and the best feasible solution x_v^{i,K^*} of problem P up to iteration K, scaling the step-size α_v^{ij} in [0,1] (Eq. (25)), and finally obtaining the trust-region radius Δ_v^{ij} (Eq. (26)). The larger the deviation of the linking variables, the greater the corresponding trust-region radius.

$$\alpha_v^{ij} := \frac{\left(\left|x_v^{i,K^*} - x_v^{i,K}\right| + \left|x_v^{j,K^*} - x_v^{j,K}\right|\right)}{\sum_{i'=1, \ j'>i'}^{S} \left(\left|x_v^{i',K^*} - x_v^{i',K}\right| + \left|x_v^{j',K^*} - x_v^{j',K}\right|\right)} \tag{25}$$

$$\Delta_v^{ij} := \alpha_v^{ij}\left|\frac{\mathrm{UB}-\mathrm{LB}}{x_v^{j,K}-x_v^{j,K}}\right| \tag{26}$$

where UB is the tightest upper bound z_λ^{LD} found at iteration K from the Lagrangean relaxation of P', and LB is the best known solution to the MIQCQP at iteration K, as explained next.

4.3. Lower bounding problem

The original problem P features binary variables and bilinear terms between continuous variables in the objective function and constraints. The classical approach to determining a lower bound on the optimal solution value of P entails fixing the values of the binary variables and solving the resulting QCQP subproblem to local optimality with a suitable initialization. Any feasible solution of this subproblem yields a lower bound z^{PF} on P. In practice, one may set the binary variables and initialize the continuous variables at the solution point of a MILP relaxation of P, constructed for instance from linear or piecewise-linear relaxations of the bilinear terms. This procedure has been successfully applied to a variety of scheduling and planning problems dealing with petroleum refineries (Castro, 2016; Mouret et al., 2011; Uribe-Rodriguez et al., 2020; Zhang et al., 2022, 2021). Nevertheless, if the bounds on the variables participating in bilinear terms are wide, the MILP relaxation may be weak and provide poor initial points for solving the QCQP subproblem as a result.

To formulate a stronger convex relaxation, the decomposable structure of P into S subproblems can be exploited. By construction, the global solution value $z_\lambda^{i,\mathrm{LD}^*}$ of each subproblem LD_λ^i may be used to tighten the MILP relaxation of P (Karuppiah and Grossmann, 2008). It is applied herein by taking advantage of the Lagrangean dual problem solution to strengthen the piecewise-linear relaxations. Incidentally, the solution value z^{R} of any such MILP relaxation also provides an upper bound on P.

4.4. Lagrangean decomposition algorithm and numerical solution

The main steps of the Lagrangean decomposition algorithm for solving the MIQCQP problem P are summarized below:

Step 1: Specify the tuning parameters, including total maximal runtime (TotalMaxRunTime), maximal runtime (MaxRunTime) for solving each subproblem, relative optimality tolerance ϵ for the Lagrangean decomposition algorithm, relative optimality tolerance ϵ^{rel} for each Lagrangean relaxation subproblem, and maximum number of iterations $K^{\max}$. Set the lower bound $\mathrm{LB} = -\infty$, the upper bound $\mathrm{UB} = +\infty$, the initial values for the Lagrange multipliers $\lambda_v^{ij,0} = 0$, and the iteration counter $K = 1$.

Step 2: Search for a feasible solution z^* (primal bound) of problem P. If successful, set $LB \leftarrow z^*$.

Step 3: Solve the S subproblems LD_λ^i with the current Lagrange multipliers $\lambda_v^{ij,K}$ to global optimality with relative tolerance ϵ^{rel} and maximal runtime MaxRunTime. Set each $z_\lambda^{i,\mathrm{LD}}$ to the best-possible solution (dual bound) of LD_λ^i at termination. If $z_\lambda^{\mathrm{LD}} = \sum_{i=1}^{S} z_\lambda^{i,\mathrm{LD}} < \mathrm{UB}$, update $\mathrm{UB} \leftarrow z^{\mathrm{R}}$.

Step 4: Append a new cut from the solution $z_\lambda^{i,\mathrm{LD}^*}$ of the Lagrangean dual problems LD_λ^i to the MILP relaxation of problem P and solve it by passing the optimal values for the continuous variables x^j and the discrete variables y^j from the S subproblems LD_λ^i as hint (choosing values from one of the subproblems for the duplicated variables). If $z^{\mathrm{R}} < \mathrm{UB}$, update $\mathrm{UB} \leftarrow z^{\mathrm{R}}$.

Step 5: Solve problem P to local optimality, by fixing the binary variables and initializing the continuous variables at the solution of the MILP relaxation in Step 4. If successful and $z^{\mathrm{PF}} > \mathrm{LB}$, update $\mathrm{LB} \leftarrow z^{\mathrm{PF}}$.

Step 6: If $(\mathrm{UB}-\mathrm{LB})/\mathrm{UB} \le \epsilon$, terminate.

Step 7: Update the trust-region radius Δ_v^{ij} using Eqs. (25)-(26).

Step 8: Solve problem DP^K to determine the next Lagrange multipliers $\lambda_v^{ij,K}$.

Step 9: If TotalMaxRunTime is exceeded or $K = K^{\max}$, terminate. Otherwise, set $K = K+1$ and return to Step 3.

The Lagrangean decomposition algorithm was implemented in the modeling environment GAMS (ver. 33.2), setting a relative optimality tolerance $\epsilon = 0.05$ and allowing for a maximal runtime TotalMaxRunTime of 36,000 s. Step 2 of the algorithm relies on the local solver DICOPT (Viswanathan and Grossmann, 1990) to find a feasible solution to problem P. In step 3, the S subproblems are solved with either of the global solvers ANTIGONE (ver. 1.1) or BARON (ver. 20.10.16), or using the process clustering decomposition approach by Uribe-Rodriguez et al. (2020), with an optimality gap $\epsilon^{\mathrm{rel}} = 0.1$ and a maximal runtime MaxRunTime of 1000 s. In step 4, the MILP relaxations are solved using CPLEX (ver. 12.8) running in parallel deterministic mode, with a relative tolerance of 10^{-4}; the initialization values for the subset of complicating variables x^j are taken from the last Lagrangean relaxation subproblem LD_λ^i solved. In step 5, the QCQP solver used to determine locally optimal solutions to problem P is CONOPT 3 (ver. 3.17 L) with an optimality tolerance of 10^{-7}.

All the computations were conducted on a 64-bit desktop virtual azure machine with an Intel Xeon platinum 8272 CL CPU @2.60 GHz, 16 cores, 32 logical processors, with 64 GB of RAM, running Windows 7.

5. Computational results

The performance of the Lagrangean decomposition algorithm to solve the short-term planning problem of one representative IRPC in Colombia is assessed on four realistic scenarios and benchmarked against the process clustering decomposition approach (CL) by Uribe-Rodriguez et al. (2020) and the commercial deterministic global solvers BARON and ANTIGONE. It is noteworthy that local solvers such as SBB and DICOPT are unable to solve this IRPC planning problem reliably. Even finding a feasible solution is heavily reliant upon supplying suitable starting values for the operating conditions, flowrates and stream properties—refer to Section 6 of the Electronic Supplementary Information for further discussions.

5.1. Scenario definition

The base-case scenario (BCS) considers: hydrocarbon market requirements for LPG, gasoline, medium distillate, fuel oil and asphalt of 15, 183, 149, 80 and 7.2 kbbl/day, respectively; combined demand for liquid petrochemicals, industrial solvents, waxes and propylene of 13.90 kbbl/day; polyethylene demand equal to 0.96 kton/day. The corresponding MIQCQP model comprises 6975 equations, 35,104 bilinear terms, 9592 continuous variables, and 279 discrete variables.

The second scenario (WRPS) omits the petrochemical processes, by setting the demands for petrochemicals, industrial solvents and waxes to zero.

The third scenario (LDS) analyzes the impact of a disruption in the domestic crude supply, by halving the capacity of pipeline system PL3, responsible for delivering up to 80% of the crude to the refinery.

The fourth scenario (DRS) analyzes the effect of reducing gasoline demand by 25%, as a means of forcing the refinery to shift production towards other commodities since the main income in BCS is dominated by gasoline and medium distillate production.

5.2. Comparison of Lagrangean decomposition with other solution strategies

For each scenario, Table 3 summarizes the computational performance of the Lagrangean decomposition (LD) algorithm from Section 4, for the two- (CM-RPB), three- (CM-RB-PTQ) and four-section (CM-REF-PTQ-FB) decompositions that were described in Section 3. Results for BARON, ANTIGONE and the clustering decomposition approach by (Uribe-Rodriguez et al., 2020) using either 2 (CL2: crude management, RPB) or 6 clusters (CL6: crude management, crude distillation, vacuum and debutanizer, refining, petrochemical production, fuel blending) are also reported.

The main benefits afforded by Lagrangean decomposition come from

Table 3
Results from spatial Lagrangean decomposition algorithm with two sections (CM-RPB), three sections (CM-RB-PTQ) and four sections (CM-REF-PTQ-FB), compared with the commercial deterministic global solvers BARON and ANTIGONE and with the process clustering decomposition approach by Uribe-Rodriguez et al. (2020) with two clusters (CL2) and six clusters (CL6). The tightest bounds and lowest gaps are indicated in bold.

	Base case scenario (BCS)			
	LB [kUSD/day]	UB [kUSD/day]	Opt Gap [%]	Runtime [h]
CM-RPB	2911	**2982**	**2.4%**	0.19
CM-RB-PTQ	2953	3181	7.2%	10.03
CM-REF-PTQ-FB	2711	3379	18.8%	10.00
ANTIGONE	2634	3898	32.4%	10.00
BARON	2684	4505	40.4%	10.00
CL2	2924	3458	15.4%	1.35
CL6	**2964**	3205	7.5%	5.70
	Without refinery-petrochemical integration scenario (WRPS)			
	LB [kUSD/day]	UB [kUSD/day]	Opt Gap [%]	Runtime [h]
CM-RPB	1943	2029	4.2%	9.40
CM-RB-PTQ	2006	**2022**	**0.8%**	0.72
CM-REF-PTQ-FB	1757	2615	32.8%	10.00
ANTIGONE	1219	2926	58.3%	10.00
BARON	1574	3536	55.5%	10.00
CL2	1970	2310	14.7%	2.46
CL6	**2009**	2233	10.0%	5.84
	Logistic disruption scenario (LDS)			
	LB [kUSD/day]	UB [kUSD/day]	Opt Gap [%]	Runtime [h]
CM-RPB	2637	**2668**	**1.2%**	0.42
CM-RB-PTQ	2661	2814	5.4%	10.08
CM-REF-PTQ-FB	2457	2848	13.7%	10.00
ANTIGONE	2156	3451	37.5%	10.00
BARON	2473	3981	37.9%	10.00
CL2	2625	3220	18.5%	0.86
CL6	**2664**	3050	12.7%	3.68
	Demand reduction scenario (DRS)			
	LB [kUSD/day]	UB [kUSD/day]	Opt Gap [%]	Runtime [h]
CM-RPB	2801	2998	6.6%	10.12
CM-RB-PTQ	2804	**2908**	**3.6%**	5.84
CM-REF-PTQ-FB	2464	2961	16.8%	10.00
ANTIGONE	2186	3719	41.2%	10.00
BARON	2478	4214	41.2%	10.00
CL2	2820	3133	10.0%	2.54
CL6	**2833**	3090	8.3%	5.80

considerably tighter dual bounds (UB) compared to the other algorithms, irrespective of the scenario considered. This translates into much smaller optimality gaps at termination: optimality gaps between 0.8 and 7.2% with either two or three sections, compared to optimality gaps between 10 and 18.5% with CL2 and 7.5–12.7% with CL6. In particular, the ability to guarantee a feasible solution around 1% of the global optimum for the WRPS and LDS scenarios is a remarkable result for such large-scale problems. The two- and three-section decompositions are also found to outperform the one using four sections, for reasons that will be discussed later on.

By contrast, none of the LD schemes can improve on the best feasible solutions (LB) found by the six-cluster decomposition (CL6). The best-found solutions from LD with two sections (CM-RPB) are comparable to those computed by the cluster decomposition with two clusters (CL2, maximal difference around 1% across all scenarios). Similarly, the best-found solutions from LD with 3 sections (CM-RB-PTQ) are comparable to those from CL6 (maximal difference around 1% across). This comparison also reveals that the MILP relaxation from the cluster decomposition algorithm can provide better starting points to the local QCQP solver than its LD counterpart (step 4), thus suggesting that the spatial Lagrangean decomposition would benefit from a more effective search for high-quality feasible solutions.

5.3. Analysis of Lagrangean decomposition strategies

The tradeoff in decomposing the large-scale MIQCQP into S subproblems (LD_s^i) is that as the subproblems (either QCQP or MIQCQP) become smaller in size, they can usually be solved to global optimality more efficiently, but this comes at the cost of more iterations in the LD algorithms since a greater number of Lagrange multipliers need to be updated simultaneously. Here, the two-section decomposition (Fig. 3) involves a total of 57 Lagrange multipliers (8 flowrates, 24 bulk properties, and 25 compositions); the disaggregation of the petrochemical plant from the refinery and fuel blending in the three-section decomposition (Fig. 4) adds 20 Lagrange multipliers (6 flowrates and 14 properties), bringing the total to 77; and the disaggregation of the fuel blending from the refinery in the four-section decomposition (Fig. 5) adds another 239 Lagrange multipliers (88 flowrates and 151 properties), leading to a grand total of 316.

The ability to solve the corresponding Lagrangean relaxation subproblems to global optimality within the 1000 s time-limit on the current platform is summarized in Table 4. The QCQP subproblem for the CM section can be globally optimized using BARON or ANTIGONE, and so can the QCQP subproblem for the FB section and the MIQCQP subproblem for PTQ. By contrast, the large-scale MIQCQP subproblem for REF alone in the four-section decomposition remains intractable within the set time-limit, and those for the aggregated RPB and RB in the two- and three-section decompositions are intractable as well. In order to

Table 4
Subproblems for the spatial Lagrangean decomposition.

S	Subproblems	Model type	Solved to global optimality? *	# Clusters in CL approach
2	**CM**	QCQP	Yes	–
	RPB	MIQCQP	No	5
3	**CM**	QCQP	Yes	–
	RB	MIQCQP	No	4
	PTQ	MIQCQP	Yes	–
4	**CM**	QCQP	Yes	–
	REF	MIQCQP	No	3
	FB	QCQP	Yes	–
	PTQ	MIQCQP	Yes	–

* By ANTIGONE and BARON.

increase the likelihood of finding a global optimum for the most challenging MIQCQPs, a cluster-decomposition approach was applied as part of the LD algorithm, using five clusters (crude distillation, vacuum and debutanizer, refining, petrochemical production, fuel blending) in the two-section case, four clusters (crude distillation, vacuum and debutanizer, refining, fuel blending) in the three-section case, and three clusters (crude distillation, vacuum and debutanizer, refinery) in the four-section case; see Uribe-Rodriguez et al., 2020 for further details about these clusters.

The performance of a Lagrangean decomposition with four sections (CM-REF-PTQ-FB) is illustrated on Fig. 7 (left plot) for the base-case scenario (BCS). While the best-found solution (LB) is about constant throughout the iterations, the dual bound (LD) from the Lagrangean decomposition and relaxation presents spurious variations. This is due to large variations in the Lagrange multiplier values, some even taking negative values (cf. right plot of Fig. 7), despite adapting the trust-region radius prior to solving the dual problem (DP^K). Overall, the presence of over 300 linking variables between all four sections requires many iterations for the dual bound to progress, which overwhelms the benefit of having smaller, more tractable subproblems in the Lagrangean relaxation. Still, as discussed in Section 5.2, the final dual bound (UB) is considerably tighter than that from commercial solvers for all four scenarios (recall Table 3). From a practical viewpoint, these variations highlight the challenges of finding an optimal compromise between the four sections: FB seeks to meet the fuel demands with cheaper high-quality materials traded with REF, while buying as little as possible from PTQ; CM seeks to sell expensive or low-quality crude blends to REF; PTQ seeks to buy cheap natural gas, virgin naphtha, olefins and ethylene from REF; while REF acts as an adversary that seeks to maximize its revenue from selling intermediates to FB and PTQ and procuring crude blends from CM. Competing against CM, FB and PTQ makes it difficult for REF to raise its profit, thereby operating at the lowest level of charge (100 kbbl/day) .

The coordination of either two (CM-RPB) and three (CM-RB-PTQ) sections in the Lagrangean decomposition also results in large variations of the dual bound (LD) and the Lagrange multipliers associated with the linking variables. However, in all the scenarios (BCS & LDS with 2 sections, WPRS & DRS with 3 sections, cf. Table 3) the Lagrangean decomposition terminates upon reaching the 5% optimality tolerance after a few dozen iterations. This success is attributed to the much smaller number of multipliers compared to the four-section decomposition.

For illustration, the performance of a Lagrangean decomposition with two sections is presented on Fig. 8 (left plot) for the base-case scenario. Recall that the Lagrange multipliers may be interpreted as transfer prices between the crude management (CM) and the integrated refinery-petrochemical complex (RPB). Important findings while searching for an optimal compromise are the following:

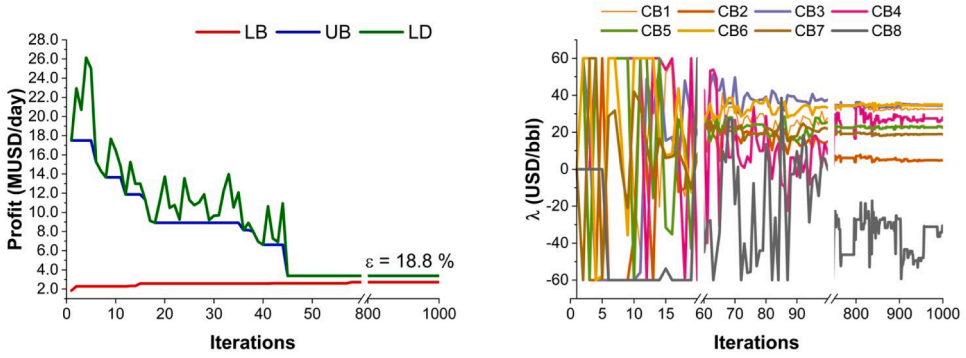

Fig. 7. Performance of the Lagrangean decomposition with four sections (CM-REF-FB-PTQ) in the base-case scenario (BCS) up to a maximal runtime of 36,000 s (left) and corresponding evolution of the Lagrange multipliers for the crude blend flowrates (right).

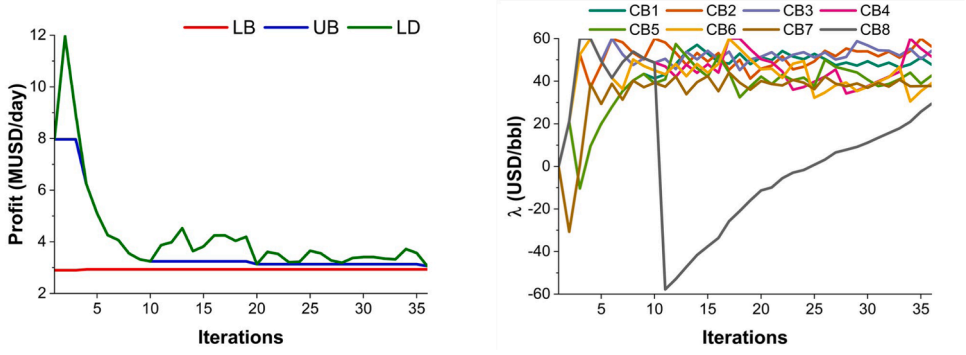

Fig. 8. Performance of the Lagrangean decomposition with two sections (CM-RPB) in the base-case scenario (BCS) up to a maximal runtime of 36,000 s (left) and corresponding evolution of the Lagrange multipliers for the crude blend flowrates (right).

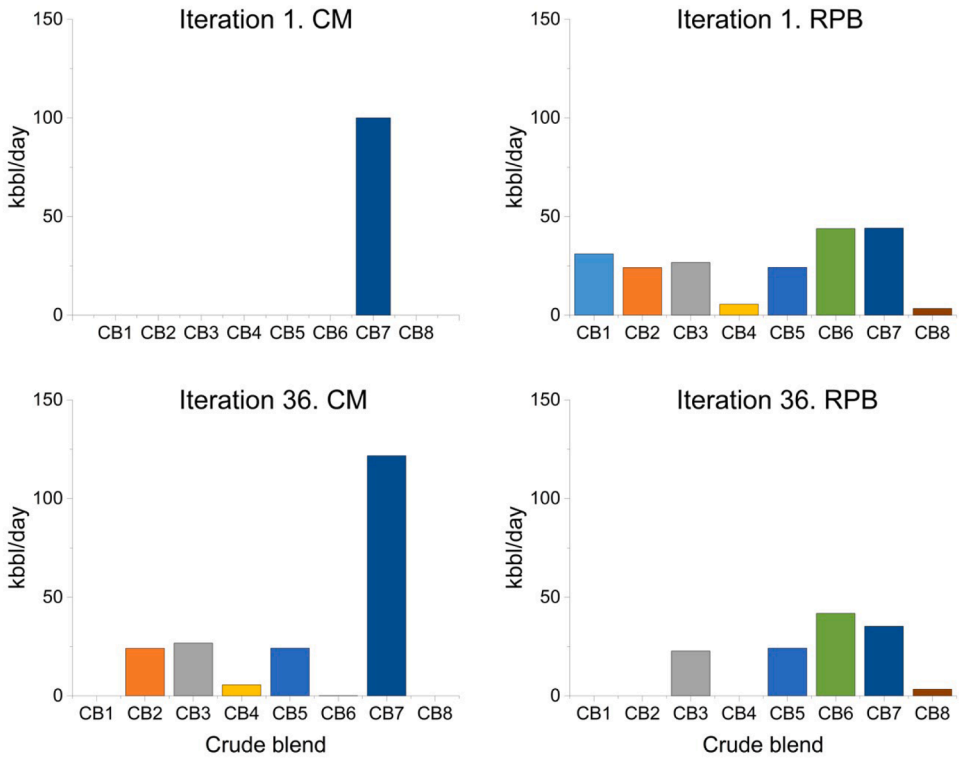

Fig. 9. Crude blend flowrates provided by CM (left) and processes by RPB (right) at iterations 1 (top) and 36 (bottom) of the Lagrangean decomposition algorithm in the base-case scenario (BCS).

- At iteration 1 with all the multipliers set to zero, CM and RPB are essentially uncoordinated, and their mismatch does not incur any penalty on the other section. CM chooses to only provide 100 kbbl/day (the minimal flow) of the crude blend CB7 (top-left plot of Fig. 9), which is comprised of 72% of domestic crude DC9, 16% of DC16, and 12% of DC17. It uses all available DC16 and DC17, which are the cheapest domestic crudes, neglecting importing crudes as they are more expensive (cf. Table 1), to achieve a minimal loss of 3.46 MUSD/day. As a result, the crude oils are heavy, sour and acid, leading to a poor-quality crude blend (20 API, 1.13%wt. sulfur content, 2.7 TAN) that fails to comply with CDU specifications. By contrast, RPB chooses to process all possible crude blends in the basket, for a total refinery capacity of 203 kbbl/day (top-right plot of Fig. 9), and achieves a maximal profit of 11.43 MUSD/day. The blends CB6 and CB7 comprise a large amount of high-quality domestic and imported crudes, which are compliant with the CDUs maximum limits of 1.2%wt. and 2.0 TAN. This strategy is expected insofar as there is no premium for processing these higher-quality crude blends. Accordingly, the initial dual bound (UB) at iteration 1 is highly conservative.
- The Lagrange multiplier values are very volatile during the first few iterations, where a fast reduction in the dual bound (UB) is observed. Following this initial phase, the multipliers of the crude blends CB1 – CB7 stabilize between 30 and 60 USD/bbl, the lowest value corresponding to the medium crude CB7 and the highest value to the light crude CB2. The Lagrange multiplier for CB8 is by far the most volatile, remaining negative between iterations 11–26, mainly due to the low fraction of this blend in the crude basket.
- At the final iteration 36, CM procures 202 kbbl/day of a basket of medium crude blends (26 API, 0.89%wt. sulfur and 1.87 TAN) that already meet the quality specifications of the CDUs (cf. bottom-left plot of Fig. 9). Meanwhile, RPB has a significantly lower throughput of 127 kbbl/day compared to iteration 1, consisting of a medium crude blend with 29 API, 0.81%wt sulfur and 0.67 TAN, which is of better quality than the crude blend provided by CM (cf. bottom-right plot of Fig. 9). With all the Lagrange multipliers – that is, trading prices – now being positive (cf. top section of Table 5), CM makes a profit of 0.73 MUSD/day, while the profit of RPB decreases to 2.25 MUSD/day (cf. middle & bottom sections of Table 5), which is within 0.6% of the best strategy found for BCS (cf. Table 3).

Table 5
Update of Lagrange multipliers, profit and throughput for CM and RPB at iterations 1 and 36 of BCS.

	Lagrange Multiplier	
	Iter#1	Iter#36
CB1	–	47.11
CB2	–	55.56
CB3	–	53.50
CB4	–	50.86
CB5	–	41.45
CB6	–	39.70
CB7	–	38.41
CB8	–	30.12
	Profit (MUSD/day)	
	Iter#1	Iter#36
CM	−3.456	0.732
RPB	11.425	2.249
	Capacity (kbbl/day)	
	Iter#1	Iter#36
CM	100	202
RPB	203	127

Overall, these results establish that Lagrangean decomposition is effective at tightly bracketing the global solution value of large-scale IRPC planning problems. They also suggest a large potential for reducing the number of iterations through improving the Lagrange multiplier update in the dual problem.

6. Conclusions

Through this paper, a spatial Lagrangean decomposition approach has been investigated to globally optimize large-scale MIQCQP problems arising in short-term planning of integrated refinery-petrochemical complexes. Such problems have not yet been addressed in their full complexity in the literature, remaining intractable to generic global optimization solvers.

To obtain more manageable QCQP and MIQCQP subproblems, different Lagrangean decomposition strategies have been formulated, which subdivide the IRPC into two, three or four sections. Such Lagrangean decompositions are akin to creating a virtual market for trading the crude blends and other intermediate refined-petrochemical streams between the different sections. The marginal prices associated with the flows and properties of these connecting streams correspond to the Lagrange multipliers in the decomposition, thus enabling a clear interpretation of the results.

A comparison on an IRPC arising from the Colombian petroleum industry for four real-life scenarios has shown that Lagrangean decomposition could reach optimality gaps between 0.8 and 7.2% with either two or three sections, even guaranteeing a near optimal solution (around 1% gap) in two scenarios. This level of performance is unprecedented and a significant improvement over cluster-decomposition algorithms that rely on piecewise-linear relaxations. A trade-off could also be identified between the number of sections and the number of iterations required by the Lagrangean decomposition algorithm, which causes the four-section decomposition to be outperformed by its two- and three-section counterparts.

Future work on the Lagrangean decomposition algorithm should focus on improving the dual problem formulation in order to handle a large number of Lagrange multipliers within a reasonable number of iterations. The algorithm would also benefit from a more effective search for feasibility or locally optimal solutions during the iterations. On the application side, a future research direction entails the integration of refinery-petrochemical short-term planning with crude oil scheduling operations, another challenging problem for which effective global optimization algorithms still need to be developed.

CRediT authorship contribution statement

Ariel Uribe-Rodríguez: Conceptualization, Methodology, Software, Investigation, Visualization, Writing – original draft, Writing – review & editing. **Pedro M. Castro:** Conceptualization, Writing – review & editing, Supervision. **Gonzalo Guillén-Gosálbez:** Conceptualization, Writing – review & editing, Supervision. **Benoît Chachuat:** Conceptualization, Writing – review & editing, Supervision.

Declaration of Competing Interest

The authors declare that they have no known competing financial interests or personal relationships that could have appeared to influence the work reported in this paper.

Data Availability

The data that has been used is confidential.

Acknowledgments

The authors would like to acknowledge financial support from the Colombian Science Council (COLCIENCIAS) and the Colombian Petroleum Company (Ecopetrol S.A.). Pedro Castro gratefully acknowledges support from Fundação para a Ciência e Tecnologia through projects CEECIND/00730/2017 and UIDB/04561/2020. Benoît Chachuat gratefully acknowledges funding by the Engineering and Physical Sciences Research Council (EPSRC) under grant EP/W003317/1. The views expressed in this paper do not necessarily reflect those of Ecopetrol S.A.

Supplementary materials

Supplementary material associated with this article can be found, in the online version, at doi:10.1016/j.compchemeng.2023.108229.

References

Al-Qahtani, K., Elkamel, A., 2010. Robust planning of multisite refinery networks: optimization under uncertainty. Comput. Chem. Eng. 34, 985–995. https://doi.org/10.1016/j.compchemeng.2007.10.017.

Al-Qahtani, K., Elkamel, A., 2009. Multisite refinery and petrochemical network design: optimal integration and coordination. Ind. Eng. Chem. Res. 48, 814–826. https://doi.org/10.1021/ie801001q.

Al-Qahtani, K., Elkamel, A., 2008. Multisite facility network integration design and coordination: an application to the refining industry. Comput. Chem. Eng. 32, 2189–2202. https://doi.org/10.1016/j.compchemeng.2007.10.017.

Alattas, A.M., Grossmann, I.E., Palou-Rivera, I., 2011. Integration of nonlinear crude distillation unit models in refinery planning optimization. Ind. Eng. Chem. Res. 50, 6860–6870. https://doi.org/10.1021/ie200151e.

Alhajri, I., Elkamel, a., Albahri, T., Douglas, P.L., 2008. A nonlinear programming model for refinery planning and optimisation with rigorous process models and product quality specifications. Int. J. Oil, Gas Coal Technol. 1 (283) https://doi.org/10.1504/IJOGCT.2008.019846.

Andrade, T., Oliveira, F., Hamacher, S., Eberhard, A., 2018. Enhancing the normalized multiparametric disaggregation technique for mixed-integer quadratic programming. J. Glob. Optim. 73, 701–722. https://doi.org/10.1007/s10898-018-0728-9.

Andrade, T., Ribas, G., Oliveira, F., 2016. A strategy based on convex relaxation for solving the oil refinery operations planning problem. Ind. Eng. Chem. Res. 55, 144–155. https://doi.org/10.1021/acs.iecr.5b01132.

ASPEN Technology Inc, 2010. ASPEN P.I.M.S. System Reference (v7.2.).

Baird, C.T., 1987. Petroleum Refining Process correlations. Inc. HPI Consultants, Houston.

Baker, T.E., Lasdon, L.S., 1985. Successive Linear Programming at Exxon. Manage. Sci. 31, 264–274. https://doi.org/10.1287/mnsc.31.3.264.

Barahona, F., Anbil, R., 2000. The volume algorithm: producing primal solutions with a subgradient method. Math. Program. Ser. B 87, 385–399. https://doi.org/10.1007/s101070050002.

Bonner & Moore, 1979. RPMS (Refinery and Petrochemical System): A System Description. Bonner & Moore Management Science, Houston.

Castillo Castillo, P., Castro, P.M., Mahalec, V., 2017. Global optimization algorithm for large-scale refinery planning models with bilinear terms. Ind. Eng. Chem. Res. 56, 530–548. https://doi.org/10.1021/acs.iecr.6b01350.

Castillo Castillo, P.A., Castro, P.M., Mahalec, V., 2018. Global optimization of MIQCPs with dynamic piecewise relaxations. J. Glob. Optim. 71, 691–716. https://doi.org/10.1007/s10898-018-0612-7.

Castro, P.M., 2016. Normalized multiparametric disaggregation: an efficient relaxation for mixed-integer bilinear problems. J. Glob. Optim. 64, 765–784. https://doi.org/10.1007/s10898-015-0342-z.

Castro, P.M., 2015. Tightening piecewise McCormick relaxations for bilinear problems. Comput. Chem. Eng. 72, 300–311. https://doi.org/10.1016/j.compchemeng.2014.03.025.

Castro, P.M., Grossmann, I.E., 2014. Optimality-based bound contraction with multiparametric disaggregation for the global optimization of mixed-integer bilinear problems. J. Glob. Optim. 59, 277–306. https://doi.org/10.1007/s10898-014-0162-6.

Castro, P.M., Liao, Q., Liang, Y., 2021. Comparison of Mixed-Integer Relaxations With Linear and Logarithmic Partitioning Schemes For Quadratically Constrained problems, Optimization and Engineering. Springer US. https://doi.org/10.1007/s11081-021-09603-5.

Cheney, E.W., Goldstein, A.A., 1959. Newton's method for convex programming and Tchebycheff approximation. Numer. Math. 1, 253–268. https://doi.org/10.1007/BF01386389.

Demirhan, C.D., Boukouvala, F., Kim, K., Song, H., Tso, W.W., Floudas, C.A., Pistikopoulos, E.N., 2020. An integrated data-driven modeling & global optimization approach for multi-period nonlinear production planning problems. Comput. Chem. Eng. 141, 107007 https://doi.org/10.1016/j.compchemeng.2020.107007.

Fisher, M.L., 1981. The lagrangian relaxation method for solving integer programming problems. Manage. Sci. 27, 1–18. https://doi.org/10.1287/mnsc.27.1.1.

Geddes, R.L., 1958. A general index of fractional distillation power for hydrocarbon mixtures. AIChE J. 4, 389–392. https://doi.org/10.1002/aic.690040403.

Gilbert, R.J.H., Leather, J., Ellis, J.F.G., 1966. The application of the Geddes fractionation index to crude distillation units. AIChE J. 12, 432–437. https://doi.org/10.1002/aic.690120309.

Gounaris, C.E., Misener, R., Floudas, C.A., 2009. Computational comparison of piecewise-linear relaxations for pooling problems. Ind. Eng. Chem. Res. 48, 5742–5766. https://doi.org/10.1021/ie8016048.

Grossmann, I.E., 2021. Advanced Optimization for Process Systems Engineering. Cambridge University Press. https://doi.org/10.1017/9781108917834.

Guerra, O.J., Le Roux, G.A.C., 2011a. Improvements in petroleum refinery planning: 1. Formulation of process models. Ind. Eng. Chem. Res. 50, 13403–13418. https://doi.org/10.1021/ie200303m.
Guerra, O.J., Le Roux, G.A.C., 2011b. Improvements in petroleum refinery planning: 2. Case studies. Ind. Eng. Chem. Res. 50, 13419–13426. https://doi.org/10.1021/ie200304v.
Guerra, O.J., Uribe-Rodriguez, A., Montagut, S.M., Duarte, L.A., Angarita, J.D., 2010. A solution strategy for large-scale nonlinear petroleum refinery planning models, in: Proceedings of the AIChE Annual Meeting. Salt Lake city.
Guignard, M., 2003. Lagrangean relaxation. TOP 11, 151–200. https://doi.org/10.1007/BF02579036.
Guignard, M., Kim, S., 1987. Lagrangean decomposition: a model yielding stronger Lagrangean bounds. Math. Program. 39, 215–228.
Guyonnet, P., Grant, F.H., Bagajewicz, M.J., 2009. Integrated model for refinery planning, oil procuring, and product distribution. Ind. Eng. Chem. Res. 48, 463–482. https://doi.org/10.1021/ie701712z.
Haverly, S., 2015. Generalized refining transportation marketing planning system - GRTMPS [WWW Document]. URL https://www.haverly.com/grtmps.
Held, M., Karp, R.M., 1971. The traveling-salesman problem and minimum spanning trees: part II. Math. Program. 1, 6–25. https://doi.org/10.1007/BF01584070.
Held, M., Wolfe, P., Crowder, H.P., 1974. Validation of subgradient optimization. Math. Program. 6, 62–88. https://doi.org/10.1007/BF01580223.
Jackson, J.R., Grossmann, I.E., 2003. Temporal decomposition scheme for nonlinear multisite production planning and distribution models. Ind. Eng. Chem. Res. 42, 3045–3055. https://doi.org/10.1021/ie030070p.
Jia, Z., Ierapetritou, M., 2004. Efficient short-term scheduling of refinery operations based on a continuous time formulation. Comput. Chem. Eng. 28, 1001–1019. https://doi.org/10.1016/j.compchemeng.2003.09.007.
Karuppiah, R., Grossmann, I.E., 2008. A Lagrangean based branch-and-cut algorithm for global optimization of nonconvex mixed-integer nonlinear programs with decomposable structures. J. Glob. Optim. 41, 163–186. https://doi.org/10.1007/s10898-007-9203-8.
Karuppiah, R., Grossmann, I.E., 2006. Global optimization for the synthesis of integrated water systems in chemical processes. Comput. Chem. Eng. 30, 650–673. https://doi.org/10.1016/j.compchemeng.2005.11.005.
Kelley, J.E., 1960. The cutting-plane method for solving convex programs. J. Soc. Ind. Appl. Math. 8, 703–712.
Kelly, J.D., Menezes, B.C., Grossmann, I.E., 2014. Distillation blending and cutpoint temperature optimization using monotonic interpolation. Ind. Eng. Chem. Res. 53, 15146–15156. https://doi.org/10.1021/ie502306x.
Ketabchi, E., Mechleri, E., Arellano-Garcia, H., 2019. Increasing operational efficiency through the integration of an oil refinery and an ethylene production plant. Chem. Eng. Res. Des. 152, 85–94. https://doi.org/10.1016/j.cherd.2019.09.028.
Kolodziej, S., Castro, P.M., Grossmann, I.E., 2013. Global optimization of bilinear programs with a multiparametric disaggregation technique. J. Glob. Optim. 57, 1039–1063. https://doi.org/10.1007/s10898-012-0022-1.
Kutz, T., Davis, M., Creek, R., Kenaston, N., Stenstrom, C., Connor, M., 2014. Optimizing Chevron's refineries. Interfaces (Providence). 44, 39–54. 10.1287/inte.2013.0727.
Leiras, A., Elkamel, A., Hamacher, S., 2010. Strategic planning of integrated multirefinery networks: a robust optimization approach based on the degree of conservatism. Ind. Eng. Chem. Res. 49, 9970–9977. https://doi.org/10.1021/ie100919z.
Li, J., Xiao, X., Boukouvala, F., Floudas, C.A., Zhao, B., Du, G., Su, X., Liu, H., 2016. Data-driven mathematical modeling and global optimization framework for entire petrochemical planning operations. AIChE J. 62, 3020–3040. https://doi.org/10.1002/aic.15220.
Li, W., Hui, C.W., Li, A., 2005. Integrating CDU, FCC and product blending models into refinery planning. Comput. Chem. Eng. 29 https://doi.org/10.1016/j.compchemeng.2005.05.010, 2010–2028.
López, D.C., Hoyos, L.J., Mahecha, C.A., Arellano-Garcia, H., Wozny, G., 2013. Optimization model of crude oil distillation units for optimal crude oil blending and operating conditions. Ind. Eng. Chem. Res. 52, 12993–13005. https://doi.org/10.1021/ie4000344.
López, D.C., Hoyos, L.J., Uribe, A., Chaparro, S., Arellano-Garcia, H., Wozny, G., 2012. Improvement of crude oil refinery gross margin using a NLP model of a crude distillation unit system. Comput. Aided Chem. Eng. 30, 987–991. https://doi.org/10.1016/B978-0-444-59520-1.50056-7.
Marsten, R.E., Hogan, W.W., Blankenship, J.W., 1975. Boxstep method for large-scale optimization. Oper. Res. 23, 389–405. https://doi.org/10.1287/opre.23.3.389.
McCormick, G.P., 1976. Computability of global solutions to factorable nonconvex programs: part I - Convex underestimating problems. Math. Program. 10, 147–175. https://doi.org/10.1007/BF01580665.
Méndez, C.A., Grossmann, I.E., Harjunkoski, I., Kaboré, P., 2006. A simultaneous optimization approach for off-line blending and scheduling of oil-refinery operations. Comput. Chem. Eng. 30, 614–634. https://doi.org/10.1016/j.compchemeng.2005.11.004.
Menezes, B.C., Kelly, J.D., Grossmann, I.E., 2013. Improved swing-cut modeling for planning and scheduling of oil-refinery distillation units. Ind. Eng. Chem. Res. 52, 18324–18333. https://doi.org/10.1021/ie4025775.
Misener, R., Floudas, C.A., 2014. ANTIGONE: algorithms for coNTinuous /integer global optimization of nonlinear equations. J. Glob. Optim. 59, 503–526. https://doi.org/10.1007/s10898-014-0166-2.
Misener, R., Thompson, J.P., Floudas, C.A., 2011. APOGEE: global optimization of standard, generalized, and extended pooling problems via linear and logarithmic partitioning schemes. Comput. Chem. Eng. 35, 876–892. https://doi.org/10.1016/j.compchemeng.2011.01.026.
Moro, L.F.L., Zanin, A.C., Pinto, J.M., 1998. A planning model for refinery diesel production. Comput. Chem. Eng. 22, S1039–S1042. https://doi.org/10.1016/S0098-1354(98)00209-9.
Mouret, S., Grossmann, I.E., Pestiaux, P., 2011. A new Lagrangian decomposition approach applied to the integration of refinery planning and crude-oil scheduling. Comput. Chem. Eng. 35, 2750–2766. https://doi.org/10.1016/j.compchemeng.2011.03.026.
Nasr, M.R.J., Sahebdelfar, S., Ravanchi, M., Beshelli, M., 2011. Integration of petrochemical and refinery plants as an approach to compete in hydrocarbon market [WWW Document]. URL https://www.researchgate.net/publication/268430340_Integration_of_Petrochemical_and_Refinery_Plants_as_an_Approach_to_Compete_in_Hydrocarbon_Market.
Neiro, S.M.S., Pinto, J.M., 2006. Lagrangean decomposition applied to multiperiod planning of petroleum refineries under uncertainty. Lat. Am. Appl. Res. 36, 213–220.
Neiro, S.M.S., Pinto, J.M., 2004. A general modeling framework for the operational planning of petroleum supply chains. Comput. Chem. Eng. 28, 871–896. https://doi.org/10.1016/j.compchemeng.2003.09.018.
Oddsdottir, T.A., Grunow, M., Akkerman, R., 2013. Procurement planning in oil refining industries considering blending operations. Comput. Chem. Eng. 58, 1–13. https://doi.org/10.1016/j.compchemeng.2013.05.006.
Oliveira, F., Gupta, V., Hamacher, S., Grossmann, I.E., 2013. A Lagrangean decomposition approach for oil supply chain investment planning under uncertainty with risk considerations. Comput. Chem. Eng. 50, 184–195. https://doi.org/10.1016/j.compchemeng.2012.10.012.
Puranik, Y., Sahinidis, N.V., 2017. Domain reduction techniques for global NLP and MINLP optimization. Constraints 22, 338–376. https://doi.org/10.1007/s10601-016-9267-5.
Sahinidis, N.V., 2004. BARON: a general purpose global optimization software package. J. Glob. Optim. 8, 201–205. https://doi.org/10.1007/bf00138693.
Siamizade, M.R., 2019. Global optimization of refinery-wide production planning with highly nonlinear unit models. Ind. Eng. Chem. Res. 58, 10437–10454. https://doi.org/10.1021/acs.iecr.9b00887.
Teles, J.P., Castro, P.M., Matos, H.A., 2013. Multi-parametric disaggregation technique for global optimization of polynomial programming problems. J. Glob. Optim. 55, 227–251. https://doi.org/10.1007/s10898-011-9809-8.
Uribe-Rodriguez, A., Castro, P.M., Guillén-Gosálbez, G., Chachuat, B., 2020. Global optimization of large-scale MIQCQPs via cluster decomposition: application to short-term planning of an integrated refinery-petrochemical complex. Comput. Chem. Eng. 140, 106883 https://doi.org/10.1016/j.compchemeng.2020.106883.
Viswanathan, J., Grossmann, I.E., 1990. A combined penalty function and outer-approximation method for MINLP optimization. Comput. Chem. Eng. 14, 769–782. https://doi.org/10.1016/0098-1354(90)87085-4.
Wenkai, L., Chi-Wai, H., Karimi, I.A., Srinivasan, R., 2007. A novel CDU model for refinery planning. ASIA - PACIFIC Chem. Eng. 2, 282–293. https://doi.org/10.1002/apj.20.
Wicaksono, D.S., Karimi, I.A., 2008. Piecewise MILP under- and overestimators for global optimization of bilinear programs. AIChE J. 54, 991–1008. https://doi.org/10.1002/aic.11425.
Yang, H., Bernal, D.E., Franzoi, R.E., Engineer, F.G., Kwon, K., Lee, S., Grossmann, I.E., 2020. Integration of crude-oil scheduling and refinery planning by Lagrangean decomposition. Comput. Chem. Eng. 138, 106812 https://doi.org/10.1016/j.compchemeng.2020.106812.
Zhang, J., Wen, Y., Xu, Q., 2012. Simultaneous optimization of crude oil blending and purchase planning with delivery uncertainty consideration. Ind. Eng. Chem. Res. 51, 8453–8464. https://doi.org/10.1021/ie102499p.
Zhang, J., Zhu, X.X., Towler, G.P., 2001. A level-by-level debottlenecking approach in refinery operation. Ind. Eng. Chem. Res. 40, 1528–1540. https://doi.org/10.1021/ie990854w.
Zhang, L., Yuan, Z., Chen, B., 2022. Adjustable robust optimization for the multi-period planning operations of an integrated refinery-petrochemical site under uncertainty. Comput. Chem. Eng. 160, 107703 https://doi.org/10.1016/j.compchemeng.2022.107703.
Zhang, L., Yuan, Z., Chen, B., 2021. Refinery-wide planning operations under uncertainty via robust optimization approach coupled with global optimization. Comput. Chem. Eng. 146, 107205 https://doi.org/10.1016/j.compchemeng.2020.107205.
Zhao, H., Ierapetritou, M.G., Shah, N.K., Rong, G., 2017. Integrated model of refining and petrochemical plant for enterprise-wide optimization. Comput. Chem. Eng. 97, 194–207. https://doi.org/10.1016/j.compchemeng.2016.11.020.